Marine and Petroleum Geology 146 (2022) 105960

Contents lists available at ScienceDirect

Marine and Petroleum Geology

journal homepage: www.elsevier.com/locate/marpetgeo

Late Jurassic syn-rift deposition in the Flemish Pass basin, offshore Newfoundland: Evidence for Tithonian magmatism and Appalachian-Variscan sediment sources from quantitative mineral and detrital zircon U–Pb-Hf isotope studies of Mizzen discovery strata

Luke P. Beranek [a,*], Adam Nissen [a], Sandra Murphy [a], David Grant [b], Dylan Goudie [b], Lindsay Oldham [a], Emily G. Johns-Buss [a]

[a] Department of Earth Sciences, Memorial University of Newfoundland, 9 Arctic Avenue, St. John's, Newfoundland and Labrador, A1B 3X5, Canada
[b] Core Research Equipment and Instrument Training Network, Memorial University of Newfoundland, St. John's, Newfoundland and Labrador, A1C 5S7, Canada

ARTICLE INFO

Keywords:
Detrital zircon
Provenance
Magma-poor rift
Grand banks
Flemish pass basin
Newfoundland
Quantitative mineralogy

ABSTRACT

Quantitative mineral and detrital zircon U–Pb-Hf isotope studies of syn-rift sandstone units in the Mizzen F-09 delineation well, northern Flemish Pass basin, were conducted to test competing models for Grand Banks paleogeography and Late Jurassic development of the Newfoundland-Iberia magma-poor rift system. Bodhrán formation (informal nomenclature) strata yield ca. 145–155 Ma detrital zircon grain populations that indicate a late Tithonian (146 ± 1 Ma) maximum depositional age for syn-rift fluvial to tide-modulated fluvial strata in Mizzen F-09 and evidence for Grand Banks rift magmatism to have occurred throughout the Late Jurassic. Late Tithonian tectonic subsidence and magmatism in the northern Flemish Pass basin region were coincident with the onset of necking processes and extreme crustal thinning within the Newfoundland-Iberia rift system. The chondritic to superchondritic Hf isotope compositions of Late Jurassic detrital zircon grains indicate repeated partial melting of lithospheric mantle during rift development, perhaps along master detachment faults or transfer zone systems. Bodhrán formation strata have chemically unstable minerals (plagioclase, potassium feldspar, garnet, muscovite, rutile, staurolite) and late Paleozoic to Paleoarchean detrital zircon age populations that together show provenance from Appalachian-Variscan basement and cover assemblages. A positive correlation between the abundance of metamorphic minerals and unique-aged, mid-Permian (ca. 271–280 Ma) detrital zircon grains from post-Variscan igneous rocks indicate Iberian provenance contributions to Bodhrán formation strata. The new results from Mizzen F-09 are consistent with models for WNW-directed fluvial discharge into the northern Flemish Pass basin and sediment derivation from upper Paleozoic foreland basin or cover assemblages located west of Variscan front, some which may have been stripped off Beothuk Knoll, Flemish Cap, or adjacent highlands.

1. Introduction

Passive or rifted continental margins have generally been divided into two end-member types based on morphology, tectonic evolution, and magma availability (e.g., Mutter, 1993; Tugend et al., 2020): (1) *magma-poor* rift margins, which are the sites of long-term (>100 Myr) stretching, extreme crustal thinning or hyperextension, exhumation or removal of mantle lithosphere, volumetrically minor magmatism, and post-breakup tectonism (e.g., Lavier and Manatschal, 2006; Jagoutz et al., 2007; Soares et al., 2012, 2014; Péron-Pinvidic et al., 2013; Sibuet and Tucholke, 2013; Huismans and Beaumont, 2014; Alves and Cunha, 2018; Zhao et al., 2021); and (2) *magma-rich* rift margins, which result from the upwelling of hot mantle, broadly coeval rupturing of crust and mantle lithosphere, and eruption of flood basalts (e.g., Coffin and Eldholm, 1994; Skogseid, 2001; Franke, 2013). The Newfoundland (SE Grand Banks) and Iberian conjugate margins (Fig. 1A and B) are the global type examples of magma-poor rift development and have long attracted interest from the petroleum, ocean drilling, and geodynamics communities (e.g., Enachescu, 1987; Alves et al., 2006, 2009; Tucholke and Sibuet, 2007; Welford and Hall, 2007; Deemer et al., 2009; Bronner

* Corresponding author.
E-mail address: lberanek@mun.ca (L.P. Beranek).

https://doi.org/10.1016/j.marpetgeo.2022.105960
Received 15 June 2022; Received in revised form 30 September 2022; Accepted 3 October 2022
Available online 7 October 2022

et al., 2011; Pereira et al., 2017; Nirrengarten et al., 2018; King et al., 2020). Marine seismic and targeted petrological studies have identified several architectural elements (e.g., proximal, necking, distal, outer, oceanic domains) along the Newfoundland-Iberian margins that record the stepwise, seaward migration of lithospheric extension (e.g., Boillot et al., 1980; Whitmarsh et al., 2001; Hart and Blusztajn, 2006; Lavier and Manatschal, 2006; Müntener and Manatschal, 2006; Péron-Pinvidic and Manatschal, 2009; Sandoval et al., 2019). Despite these and other advances in understanding depth-dependent stretching and thinning along North Atlantic-type margins (e.g., Huismans and Beaumont, 2011, 2014), there is comparatively less information about the stratigraphic archives of magma-poor rift evolution or the linked connections between tectonic exhumation, magmatism, and sediment routing across different architectural elements. For example, the erosion-deposition histories of Upper Jurassic to Lower Cretaceous proximal domain strata along the Newfoundland margin (e.g., Tankard and Welsink, 1987; Sinclair, 1988, 1993; Hiscott et al., 1990; all stratigraphic and numerical ages follow the time scale of Cohen et al., 2013, version 2022/2) were interpreted in the context of now-superseded rift models (e.g., Falvey, 1974; Lister et al., 1986) prior to the arrival of magma-poor rift scenarios in the literature. As a result, there is a critical need to understand the source-to-sink evolution of magma-poor rift margins and the process-response relationships between architectural elements during lithospheric extension from a modern perspective (e.g., Manatschal, 2004).

Mesozoic basins of the Grand Banks region (Fig. 1C) contain Upper Triassic to Upper Cretaceous strata that resulted from syn-rift to post-breakup processes in the proximal domain (Péron-Pinvidic et al., 2013) or thinning and necking subdomains (e.g., Nirrengarten et al., 2018; Sandoval et al., 2019) of the Newfoundland margin. The Jeanne d'Arc and Flemish Pass basins have proven petroleum systems and therefore been a focus for offshore geological and geophysical studies (e.g., Enachescu, 1987; Foster and Robinson, 1993; Shannon et al., 1995; DeSilva, 1999; Cawood et al., 2021a, 2021b). Active and prospective oil fields in these basins contain similar syn-rift, Upper Jurassic reservoir rocks that may have been laterally equivalent before the post-Early Cretaceous rise of basement ridges (e.g., Hutter and Beranek, 2020). Despite their significance to North Atlantic tectonic evolution, there is no consensus on the paleogeographic setting and provenance of syn-rift Upper Jurassic strata that now underlie deep-water regions of the Grand Banks, especially those that comprise the Mizzen discovery (Figs. 1C, 2A and 2B; e.g., Haynes et al., 2013) in the northern Flemish Pass basin. Upper Jurassic well cuttings from Mizzen L-11 (Figs. 1C, 2A and 2B) yielded Late Jurassic to Neoarchean detrital zircon grains and heavy mineral assemblages that were originally interpreted to reflect 400–500 km of east-directed sediment transport from the Newfoundland Appalachians (Lowe et al., 2011). Equivalent Upper Jurassic strata assigned to the Bodhrán formation (informal nomenclature; Haynes et al., 2013) in Mizzen L-11, O-16, and F-09 (Figs. 1C, 2A and 2B) were later proposed to comprise part of a south-to southwest-directed drainage system that sampled Paleozoic and older Appalachian-related rocks near the northwestern flank of Flemish Cap (Cody et al., 2012). Recent depositional models for the northern Flemish Pass basin have further interpreted that syn-rift strata in the Mizzen discovery had sources from the east or southeast (Beicip-Franlab, 2015), perhaps from Variscan (Hercynian) foreland basin successions outboard of the Grand Banks or late

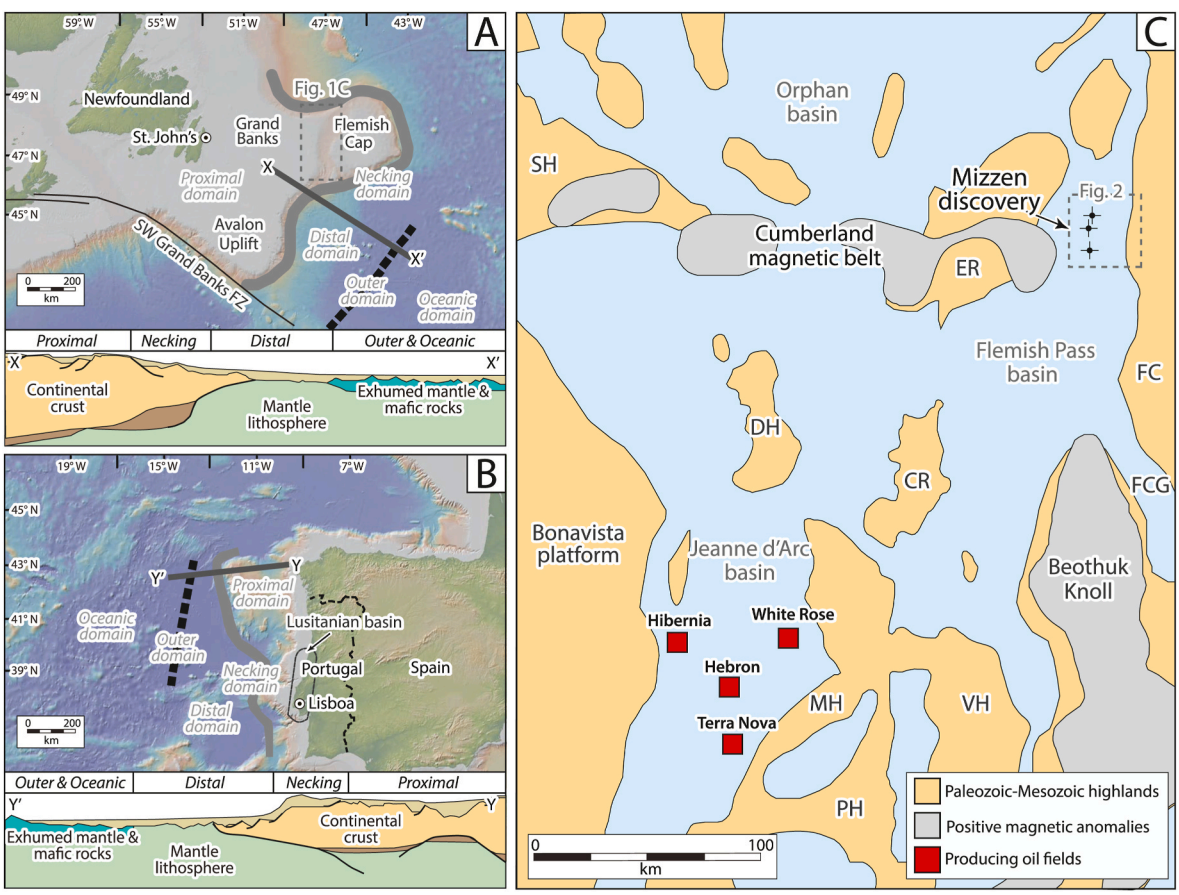

Fig. 1. Schematic maps, cross sections, and architectural elements of the (A) Newfoundland margin and (B) Iberian margin modified from Péron-Pinvidic et al. (2013) and Beranek (2017). (C) Simplified map of the northeastern Grand Banks of Newfoundland, including location of the Mizzen discovery in the northern Flemish Pass basin, modified from Cody et al. (2012). CR – Central Ridge, DH – Dominion High, ER – Eastern Ridge, FC – Flemish Cap, FCG – Flemish Cap Graben, FZ – fault zone, MH – Morgiana High, PH – Pyramid High, SH – Sheridan High, VH – Vesta Horst.

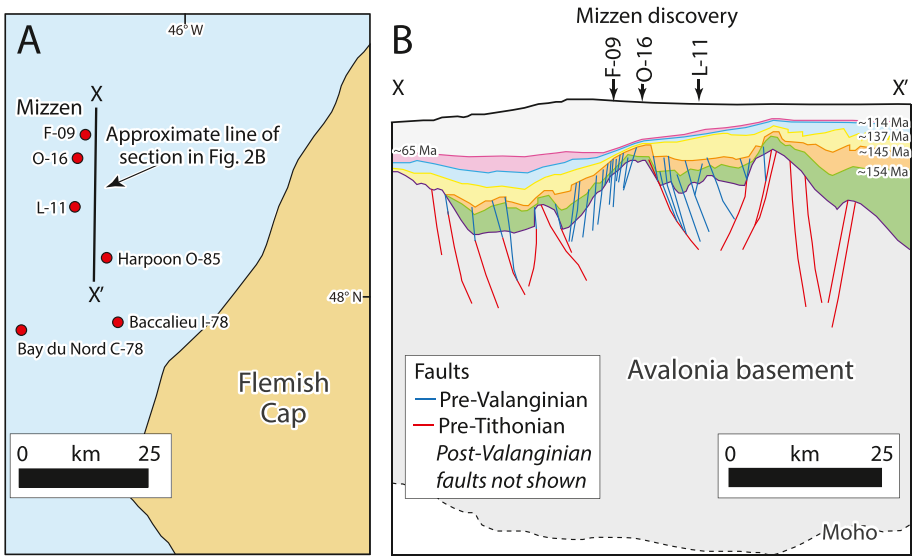

Fig. 2. (A) Simplified map of the northern Flemish Pass area with the locations of the Mizzen discovery (F-09, O-16, L-11) wells and adjacent discoveries on the western flank of Flemish Cap. (B) Cartoon north to south (X to X′) cross-section near Mizzen discovery area modified from Beicip-Franlab (2015). Vertical exaggeration ~2x.

Paleozoic intrusive rocks of the Iberian Peninsula (e.g., McDonough et al., 2011). Upper Jurassic braided fluvial units of the Jeanne d'Arc Formation in the Terra Nova oil field, Jeanne d'Arc basin (Fig. 1C), yield detrital zircon U–Pb-Hf isotope signatures that indicate southern provenance from Appalachian sources and syn-rift, Late Jurassic (ca. 145–147 Ma) volcanic centers in the Avalon Uplift region and may be correlative with some Flemish Pass basin strata (Hutter and Beranek, 2020).

In this article, we combine quantitative mineralogical and detrital zircon U–Pb-Hf isotope studies of Mizzen F-09 drillcore materials to constrain sediment provenance, test the paleogeography of the Grand Banks region, and interpret the source-to-sink responses of magma-poor rift evolution along the Newfoundland margin. New quantitative mineralogical results of Upper Jurassic strata in the Terra Nova oil field are also reported and integrated with detrital zircon U–Pb-Hf isotope constraints from Hutter and Beranek (2020). Our findings indicate that syn-rift, Bodhrán formation strata in the northern Flemish Pass basin were deposited during a late Tithonian (ca. 146 Ma) magmatic event in the Grand Banks-Iberia region and primarily sourced from local Appalachian-Variscan rock successions in the Flemish Cap and Beothuk Knoll areas to the east-southeast. The sedimentary facies and detrital zircon U–Pb-Hf isotope signatures of Bodhrán formation strata are analogous to those of the Jeanne d'Arc Formation, but likely reflect coeval sedimentation in unconnected depocenters. The results confirm that Tithonian tectonic subsidence in the northern Flemish Pass and Jeanne d'Arc basins overlapped with the onset of lithospheric necking and hyperextension processes, indicating that these strata are useful archives of long-term magma-poor rift evolution. In combination with published information, we present a revised model for Late Jurassic paleogeography in the Grand Banks region that can be tested by future studies.

2. Geological background

2.1. Newfoundland margin

Magma-poor rift stratigraphy is related to the development of architectural elements that record long-term lithospheric extension and localization of rifting toward the area of eventual breakup (e.g., Péron-Pinvidic et al., 2013; Alves and Cunha, 2018). In the Newfoundland-Iberia conjugate margin system, these elements were generated during a polyphase rift history that includes Triassic to Cretaceous extensional deformation events (e.g., Hiscott et al., 1990; Péron-Pinvidic and Manatschal, 2009) prior to lithospheric breakup (e.g., Tucholke et al., 2007; Alves et al., 2009; Soares et al., 2012). The proximal domain of the Newfoundland margin is underlain by thick (~30 km) continental crust and contains half-graben and graben basins that are the stratigraphic archives of tectonic and thermal subsidence events in the Grand Banks (Fig. 3; e.g., Hiscott et al., 1990; Lau et al., 2006; Welsink and Tankard, 2012). The proximal domain consists of basement highs, sedimented ridges, and intervening rift basins that are floored by Paleozoic and older rocks of the Appalachian orogen (Fig. 1C; e.g., Haworth and Lefort, 1979; King et al., 1985; Hiscott et al., 2008). Syn-rift, Late Jurassic to Early Cretaceous extrusive-intrusive complexes along the Newfoundland margin are rare, but recognized in the north-central Newfoundland Appalachians (Peace et al., 2018, 2019) and along the SW Grand Banks transform fault system and Collector anomaly that generally comprise the boundary between Avalonia and Meguma (Pe-Piper et al., 2007; Bowman et al., 2012). Equivalent igneous rocks have also been identified along Variscan and younger fault systems in the Lusitanian basin of Portugal (Grange et al., 2008; Mata et al., 2015; Pereira et al., 2017) and along the Iberia distal margin (Jagoutz et al., 2007).

The necking domains of the Newfoundland margin correspond with the continental slope at the edge of the Grand Banks (e.g., Péron-Pinvidic et al., 2013) and some regions of thinned crust (<20 km thick) between the Bonavista platform and Flemish Cap (e.g., Nirrengarten et al., 2018; Sandoval et al., 2019; Welford et al., 2020). Necking processes began by the Tithonian (Sutra and Manatschal, 2012; Nirrengarten et al., 2018) and overlapped with extensional deformation that generated syn-tectonic sandstone reservoir units (Fig. 3; e.g., Hiscott et al., 1990; Haynes et al., 2013). The distal or hyperextended domain is generally considered to coincide with the ocean-continent transition and in the Newfoundland rift system contains zones of serpentinized continental mantle that were exhumed by Cretaceous normal faults (e.g., Welford et al., 2010; Péron-Pinvidic et al., 2013). The distal domain outboard of the SE Grand Banks is underlain by Cretaceous and younger strata of the Newfoundland basin (Fig. 1A and B) and includes sills that provide evidence for post-breakup magmatism (Hart and Blusztajn, 2006; Soares et al., 2012). The outer domain probably contains exhumed mantle and mafic rocks that juxtapose inboard elements with oceanic domain units defining the modern ocean-continent

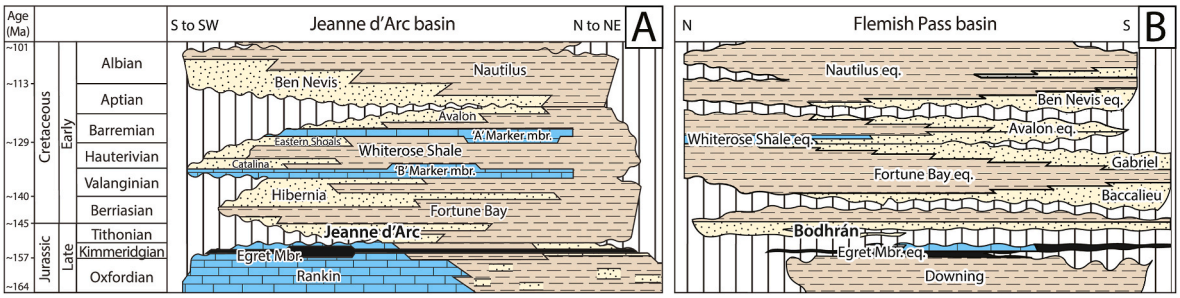

Fig. 3. Upper Jurassic to Lower Cretaceous formations of the (A) Jeanne d'Arc basin compiled from Sinclair et al. (1992) and (B) Flemish Pass basin compiled from Cody et al. (2012). The chronostratigraphic chart follows the time scale of Cohen et al. (2013, version 2022/2). Eq – equivalent, Mbr. Member.

boundary (Fig. 1A).

2.2. Flemish Pass basin and Mizzen discovery

The Flemish Pass basin is located ~500 km east of St. John's, Newfoundland and Labrador, and underlies the bathymetric saddle between the Grand Banks and Flemish Cap (Fig. 1A; e.g., Enachescu, 1987). The Flemish Pass basin is ~13,500 km^2 and separated from the adjacent Jeanne d'Arc, Orphan, and other rift basins by Mesozoic and older basement highs to the north, west, and south, respectively (Fig. 1C; e.g., Cody et al., 2012). Flemish Cap is a tethered continental ribbon that underwent clockwise rotation and dextral displacement during the Jurassic-Cretaceous opening of the eastern Orphan (e.g., Srivastava and Verhoef, 1992; Sibuet et al., 2007; Welford et al., 2010; Neuharth et al., 2021) and Flemish Pass basins (e.g., Haynes et al., 2013). Positive magnetic anomalies to the west of the northern Flemish Pass basin, represented by the Cumberland magnetic belt (Fig. 1C), comprise part of a >150 km-long volcanic chain buried by Cretaceous and younger strata (Enachescu, 1987; Sinclair, 1988). The Cumberland magnetic belt is more broadly interpreted as an east-to northeast-trending fault system that accommodated dextral strike-slip motion during Late Jurassic to Early Cretaceous transtension (e.g., Cawood et al., 2021a, 2021b). Positive magnetic anomalies and intermediate seismic velocities are characteristic of Beothuk Knoll to the southeast of the Flemish Pass basin (Fig. 1C) and may indicate buried igneous complexes (Enachescu, 1987), underplated igneous rocks, or lower crustal sills (e.g., Van Avendonk et al., 2006).

The Mizzen discovery is part of a north-trending horst block that was drilled in 2003 (Mizzen L-11), 2008 (Mizzen O-16), and 2011 (Mizzen F-09) to constrain the presence and quality of reservoir sandstone units in the northern Flemish Pass basin (Figs. 1C, 2A and 2B; e.g., Cody et al., 2012). Upper Jurassic strata assigned to the Bodhrán formation were targeted in each well and are probably equivalent to producing reservoirs at the Terra Nova oil field in the Jeanne d'Arc basin (Fig. 3; Haynes et al., 2013; Ainsworth et al., 2015). The Bodhrán formation is estimated to be > 200 m-thick and the cored interval (Ti-3 reservoir member) in Mizzen F-09 contains six lithofacies (Haynes et al., 2013): (I) poorly laminated lime mudstone; (II) matrix-supported granule to cobble conglomerate (III); planar cross-stratified sandstone (IV); planar stratified sandstone; (V) ripple cross-laminated sandstone; and (VI) interbedded shale, siltstone, and fine-grained sandstone. Based on regional stratigraphic correlations of several Tithonian reservoir members (Ti-1, Ti-2, Ti-3) across the Mizzen structure, Bodhrán formation rocks were likely parts of a syn-tectonic, fluvial-estuarine belt (Cody et al., 2012; Haynes et al., 2013).

Upper Jurassic sandstone units in the Flemish Pass basin are feldspathic to sublithic to lithic arenites that contain sedimentary, metamorphic, and igneous rock fragments and indicate diverse sources for syn-rift strata (e.g., Lowe et al., 2011; C-NLOPB, 2012; Xiong et al., 2016). Published provenance results from the northern Flemish Pass basin are restricted to Mizzen L-11, where Upper Jurassic well cuttings yield heavy mineral constituents and Mesozoic to Neoarchean detrital zircon grains that were derived from Appalachian-Variscan metasedimentary assemblages and Mesozoic rift-related igneous rocks (Lowe et al., 2011).

3. Materials and methods

Rock samples were collected at the Canada-Newfoundland and Labrador Offshore Petroleum Board Core Storage and Research Centre in St. John's, Newfoundland and Labrador (Fig. 4). The sampled intervals in Mizzen F-09 (48° 18′ 21.68″ N, 46° 15′ 52.73″ W) and Terra Nova K-18 (46° 27′ 43.73″ N, 48° 32″ 27.70″ W) were taken from fluvial, tide-modulated fluvial, and estuarine facies associations (Table 1; Haynes et al., 2013; Hutter and Beranek, 2020).

3.1. Detrital zircon U–Pb geochronology and Hf isotope geochemistry

Detrital zircon crystals were isolated from rock samples by standard rock crushing, disc milling, and methylene iodide heavy liquid separation methods, put onto double-sided tape, and mounted in epoxy. After polishing to expose the interior of the crystals, backscatter electron imaging of the mounts using a FEI MLA 650 FEG scanning electron microscope was completed at the Memorial University of Newfoundland. The images were used to locate homogeneous regions of the zircon grains and avoid complex internal structures, cracks, and zones of potential Pb loss.

Detrital zircon U–Pb-Hf isotope analyses were conducted using the laser ablation split-stream technique (e.g., Fisher et al., 2014; Beranek et al., 2020; Hutter and Beranek, 2020) at Memorial University of Newfoundland. Detrital zircon results and reference material values are reported in Appendix A (Table S1). Zircon crystals were ablated with a GeoLas 193 nm excimer laser ablation system using a 40 μm spot-size, laser fluence of 5 J/cm^2, pulse rate of 10 Hz, and 600 shots with a total analysis time of approximately 120 s (~30 s background measurement, ~60 s ablation, and ~30 s washout). Crystals that could not accommodate a 40 μm spot were not analyzed. Ablated material was evacuated from the ablation chamber via He carrier gas and split using a baffled Y-connector. The Hf isotopes were acquired using a ThermoFinnigan NEPTUNE multi-collector-inductively coupled plasma-mass spectrometer (ICP-MS) and U–Pb isotopes were measured using a ThermoFinnigan ELEMENT XR magnetic sector ICP-MS. Time-integrated U–Pb signals were analyzed offline using Iolite software (Paton et al., 2011). Age calculations were made using the VizualAge DRS, which includes a correction routine for down-hole fractionation (Petrus and Kamber, 2012). Time-resolved mass-204 signal intensities were evaluated in Iolite and therefore no common Pb correction was applied (e.g., Matthews and Guest, 2016; Fisher et al., 2017). U–Pb ages were calibrated to the 1065 Ma zircon standard 91500 (Wiedenbeck et al., 1995) and ^{176}Hf/^{177}Hf ratios were compared to those of the 337 Ma zircon standard Plešovice (Sláma et al., 2008). Secondary reference materials 02123 (Ketchum et al., 2001) and

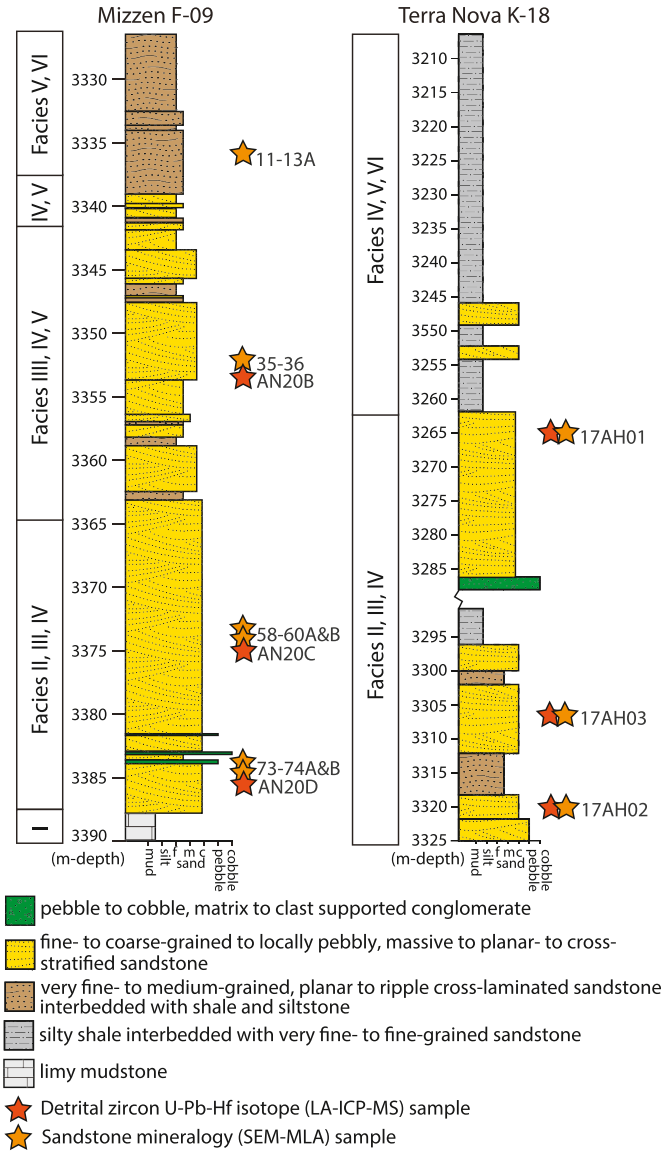

Fig. 4. Upper Jurassic stratigraphy and rock sample locations in Mizzen F-09 and Terra Nova K-18. Note different vertical scales in the two columns. f – fine sand, m – medium sand, c – coarse sand.

Temora2 (Black et al., 2004; Fisher et al., 2014) were used to monitor instrument drift. Concordance values were calculated as the ratio of $^{206}Pb/^{238}U$ and $^{207}Pb/^{206}Pb$ ages and analyses with high error (>10% uncertainty) or excessive discordance (>10% discordant, >5% reverse discordant) were excluded from plots and interpretation. The reported ages for grains younger and older than 1200 Ma are based on $^{206}Pb/^{236}U$ and $^{207}Pb/^{206}Pb$ ages, respectively.

U–Pb dates are reported at 2σ uncertainty and presented in probability density plots (PDPs) made with the DZmnf MATLAB program of Saylor et al. (2019). Age peaks were determined with the AgePick Excel macro from the Arizona Laserchron Centre (www.laserchron.org). Initial $^{176}Hf/^{177}Hf$ ratios are reported as $\varepsilon Hf_{(t)}$ and represent isotopic compositions at the time of crystallization relative to the chondritic uniform reservoir (CHUR). Initial epsilon Hf ($\varepsilon Hf_{[t]}$) calculations used the decay constant of Söderlund et al. (2004) and present-day CHUR values of Bouvier et al. (2008). The uncertainties for each Hf isotope analysis ranged from 0.4 to 1.8 epsilon units, with an average value of 0.8 epsilon units. Age-corrected epsilon Hf ($Hf_{[t]}$) vs. U–Pb age plots were made with the Hafnium Plotter MATLAB program of Sundell et al. (2019). The Maximum Likelihood Age IsoplotR routine of Vermeesch (2021) was used to estimate maximum depositional ages. Statistical comparisons (Cross-correlation, Likeness, and Similarity coefficients of PDPs, Kolmogorov-Smirnov and Kuiper tests) were conducted with the DZstats MATLAB program of Saylor and Sundell (2016) and reported in the Appendix (Table S2). Multi-dimensional scaling (MDS) plots were constructed with the DZmds MATLAB program of Saylor et al. (2018) to compare U–Pb age results and test stratigraphic correlations.

3.2. Scanning electron microscopy – mineral liberation analysis

Quantitative mineralogical studies of 30 μm-thick, polished and coated thin sections were conducted at the MicroAnalysis Facility, Memorial University of Newfoundland using a FEI Quanta field emission gun (FEG) 650 scanning electron microscope equipped with Mineral Liberation Analysis (MLA) software version 3.14 (e.g., Gu, 2003; Sylvester, 2012; Grant et al., 2018; Feely et al., 2019). Instrument conditions included a high voltage of 25 kV, working distance of 13.5 mm, and beam current of 10 nA. SEM-MLA maps were created using GXMAP mode by acquiring Energy Dispersive X-Ray (EDX) spectra in a grid every 10 pixels, with a spectral dwell time of 12 ms, and comparing these against a list of mineral reference spectra. The MLA frames were 1.5 mm by 1.5 mm with a resolution of 500 pixels per frame. Table 1 reports the area percentage of each mineral in thin-section and shows four groups: (1) rock-forming minerals (plagioclase, potassium feldspar, quartz); (2) minor and accessory minerals (e.g., apatite, garnet, zircon); (3) secondary minerals that are the result of hydrothermal alteration or greenschist facies metamorphism (e.g., albite, chlorite) or diagenesis (e.g., ankerite, pyrite); and (4) organics and inferred porosity (glass). Representative MLA maps for each sample are reported in Appendix A (Figure S1).

4. Results

4.1. Detrital zircon U–Pb ages and Hf isotope compositions

Fine-to coarse-grained sandstone from the lowermost fluvial section (3384.60–3386.20 m) mostly yielded mid-to late Neoproterozoic (541 ± 8 Ma to 720 ± 14 Ma, 58%), early Neoproterozoic to Paleoproterozoic (793 ± 19 Ma to 1929 ± 26 Ma, 20%), and Paleozoic (271 ± 10 Ma to 471 ± 11 Ma, 17%) detrital zircon grains with main age peaks of 431, 473, 547, and 609 Ma (Fig. 5A). A minor mid-Permian subpopulation (271 ± 10 Ma to 280 ± 5 Ma, 3%) occurs in the Paleozoic age group. Subordinate Mesozoic (144 ± 5 Ma to 161 ± 8 Ma, 3%) and Neoarchean and older (>2500 Ma, 2%) detrital zircon grains were also observed.

Medium-grained sandstone to granule conglomerate from the upper fluvial section (3372.60–3375.00 m) mostly yielded mid-to late Neoproterozoic (552 ± 17 Ma to 717 ± 14 Ma, 31%), early Neoproterozoic to Paleoproterozoic (766 ± 20 Ma to 2072 ± 85 Ma, 31%), Paleozoic (300 ± 3 Ma to 522 ± 12 Ma, 22%), and Neoarchean and older (>2500 Ma, 14%) detrital zircon grains with main age peaks of 432, 456, 622, 1664, 1798, and 2726 Ma (Fig. 5B). Mesozoic (146 ± 2 Ma to 153 ± 7 Ma, 3%) detrital zircon grains form a subsidiary population.

Fine-to coarse-grained sandstone from the tide-modulated fluvial section (3350.80–3354.20 m) mostly yielded early Neoproterozoic to Paleoproterozoic (973 ± 32 Ma to 2090 ± 24 Ma, 40%), mid-to late Neoproterozoic (544 ± 16 Ma to 692 ± 24 Ma, 30%), and Paleozoic (286 ± 11 Ma to 530 ± 14 Ma, 24%) detrital zircon grains with main age peaks of 374, 417, 605, 685, 1630, and 1822 Ma (Fig. 5C). A single Mesozoic (143 ± 6 Ma) detrital zircon grain was observed.

The Hf isotope compositions of dated detrital zircon grains are shown in Fig. 5D. Mesozoic detrital zircon grains have chondritic to superchondritic isotope compositions (+1.2 to +8.1; $\overline{X}$ = +4.4), whereas older age populations generally show a range of superchondritic to subchondritic isotope compositions with mean values near CHUR: late Paleozoic (ca. 271–300 Ma, $\varepsilon Hf_{(t)}$ = −3.3 to +2.8, $\overline{X}$ = +0.7), mid-to

Table 1
Modal abundances (area%) of Tithonian sandstone units in Mizzen F-09 and Terra Nova K-18 wells. Lithofacies from Haynes et al. (2013): II, III, IV = Fluvial, III, IV, V = Tide-modulated fluvial, IV, V, VI = Estuarine.

	Mizzen F-09 (Bodhrán formation)						Terra Nova K-18 (Jeanne d'Arc Formation)		
Sample	73–74A (AN20D)	73–74B (AN20D)	58–60A (AN20C)	58–60B (AN20C)	35-36 (AN20B)	11–13A	17AH02	17AH03	17AH01
Depth (m)	3384.60–3386.20	3384.60–3386.20	3372.60–3375.00	3372.60–3375.00	3350.80–3354.20	3335.00–3337.40	3317–3323	3306–3311	3265–3271
Grain size	Fine to coarse sand	Fine to coarse sand	Medium sand to pebble	Medium sand to granule	Fine to coarse sand	Very fine to fine sand	Fine sand	Very fine to fine sand	Medium to coarse sand
Lithofacies	II, III, IV	II, III, IV	II, III, IV	II, III, IV	III, IV, V	IV, V, VI	II, III, IV	II, III, IV	II, III, IV
Rock-forming minerals									
Plagioclase	0.30	0.68	0.20	0.16	0.17	0.49	0.06	0.03	0.05
Potassium feldspar	1.40	1.35	0.45	0.29	1.02	0.86	0.09	0.07	0.08
Quartz	52.20	48.53	51.18	50.85	65.39	63.43	73.48	75.84	61.70
subtotal	53.60	49.88	51.63	51.14	66.41	64.29	73.57	75.91	61.78
Minor and accessory minerals									
Apatite	0.01	0.03	0.02	0.02	0.05	0.04	0.02	<0.01	0.02
Biotite	<0.01	<0.01	<0.01	<0.01	<0.01	<0.01	<0.01	<0.01	<0.01
Chromite	<0.01	<0.01	<0.01	<0.01	<0.01	<0.01	<0.01	<0.01	0.00
Enstatite	0	0	<0.01	0	0	0	0	0	0
Garnet	0.02	0.02	0.01	0.01	0.03	0.03	0.01	0.01	0.01
Ilmenite	<0.01	<0.01	0	<0.01	0	<0.01	<0.01	<0.01	<0.01
Magnetite	<0.01	<0.01	<0.01	<0.01	0.01	<0.01	0.01	<0.01	<0.01
Monazite	0.02	0.01	<0.01	<0.01	<0.01	<0.01	<0.01	<0.01	<0.01
Muscovite	0.38	0.49	0.13	0.10	0.08	0.27	0.01	<0.01	0.06
Olivine	<0.01	<0.01	<0.01	<0.01	0	<0.01	<0.01	<0.01	<0.01
Rutile	0.35	0.17	0.05	0.04	0.07	0.34	0.02	0.04	0.01
Rutile-Ilmenite mix	0.02	0.02	0.01	<0.01	<0.01	0.05	<0.01	<0.01	<0.01
Staurolite	0.16	0.18	0.04	0.05	0.04	0.18	0.01	0.02	0.03
Titanite	0.01	0.01	<0.01	<0.01	0.01	0.01	0.01	0.01	0.01
Zircon	0.01	0.01	<0.01	<0.01	0.01	0.04	<0.01	<0.01	<0.01
subtotal	0.98	0.94	0.26	0.22	0.30	0.96	0.09	0.08	0.14
Secondary minerals									
Albite	4.55	5.90	2.35	1.89	3.73	13.05	1.03	1.22	0.87
Ankerite	0.32	0.56	0.38	0.31	0.19	0.32	2.11	0.57	15.79
Apatite (biogenic)	0.45	1.23	0.43	0.33	0.42	0.58	0.16	0.04	0.2
Barite	<0.01	<0.01	<0.01	<0.01	<0.01	<0.01	0.01	0.01	0.01
Ba-Celestin	0.01	<0.01	<0.01	<0.01	0.01	<0.01	<0.01	<0.01	<0.01
Calcite	36.20	34.32	39.69	42.18	5.22	2.65	2.09	<0.01	15.21
Chalcopyrite	<0.01	<0.01	<0.01	<0.01	<0.01	<0.01	<0.01	<0.01	<0.01
Chlorite	0.27	0.30	0.08	0.08	0.11	0.14	0.01	0.01	0.04
Clinochlore	0	<0.01	0	0	<0.01	<0.01	<0.01	<0.01	0
Dolomite	0.07	0.10	0.12	0.06	0.05	0.14	0.05	0.02	0.34
Galena	0	<0.01	<0.01	<0.01	<0.01	0.01	<0.01	<0.01	0
Glauconite	0.32	0.34	0.15	0.14	0.26	0.42	0.07	0.06	0.09
Illite	1.66	2.16	0.95	0.78	2.02	3.22	0.58	0.41	0.59
Kaolinite	0.15	0.14	0.17	0.18	0.67	1.69	0.39	0.39	0.25
Pyrite-Rutile-Ilmenite	<0.01	0.01	<0.01	<0.01	<0.01	0.01	0	<0.01	0
Pyrite	0.17	0.31	0.31	0.3	0.61	2.88	0.1	0.02	0.05
Siderite	<0.01	<0.01	<0.01	<0.01	<0.01	<0.01	<0.01	<0.01	<0.01
Sphalerite	<0.01	<0.01	<0.01	<0.01	<0.01	<0.01	0	<0.01	<0.01
Xenotime	<0.01	<0.01	<0.01	<0.01	<0.01	<0.01	<0.01	<0.01	<0.01
subtotal	44.17	45.37	44.63	46.25	13.29	25.11	6.60	2.75	33.44
Other									
Organics	0.20	0.70	0.37	0.29	1.03	2.21	0.34	0.35	0.14
Porosity (glass)	0.76	2.41	2.90	1.90	18.79	6.93	19.32	20.88	4.45
Total	100.00	100.00	100.00	100.00	100.00	100.00	100.00	100.00	100.00

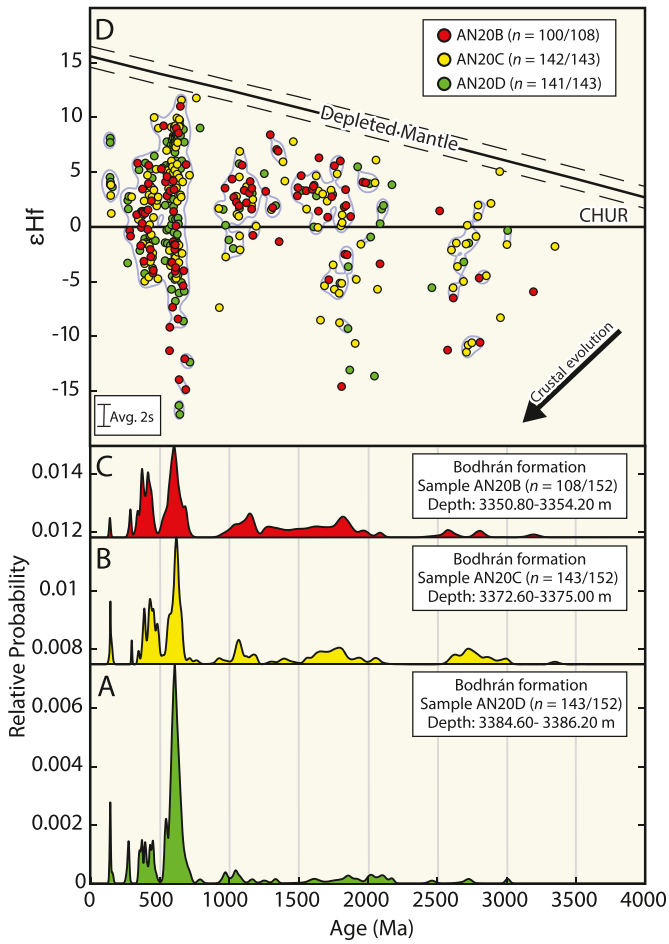

Fig. 5. Detrital zircon U–Pb-Hf isotope results for Bodhrán formation rock units in Mizzen F-09. (A) fine-to coarse-grained sandstone from the lowermost (3384.00–3386.20 m) fluvial section (sample AN20D). (B) medium-grained sandstone to granule conglomerate from the upper (3372.60–3375.00 m) fluvial section (sample AN20C). (C) fine-to coarse-grained sandstone from the lower (3350.80–3354.20 m) tide-modulated fluvial section (sample AN20B). (D) εHf(t) vs. U–Pb age diagram for Bodhrán formation samples. CHUR—chondritic uniform reservoir.

early Paleozoic (ca. 336–530 Ma, $\varepsilon Hf_{(t)} = -5.0$ to $+10.0$, $\overline{X} = +1.2$), late to mid-Neoproterozoic (ca. 541–720 Ma, $\varepsilon Hf_{(t)} = -17.1$ to $+11.8$, $\overline{X} = +2.0$), early Neoproterozoic to Paleoproterozoic (ca. 766–2464 Ma, $\varepsilon Hf_{(t)} = -14.6$ to $+11.8$, $\overline{X} = +1.0$), and Neoarchean and older (ca. 2520–3351 Ma, $\varepsilon Hf_{(t)} = -11.4$ to $+5.1$, $\overline{X} = -3.6$).

Table 2 shows the maximum depositional age results for Bodhrán formation strata from Mizzen F-09 and Jeanne d'Arc Formation in Terra Nova K-18. Age estimates are given at 2σ uncertainty (e.g., Spencer et al., 2016). The Bodhrán formation has an estimated maximum depositional age of 146 ± 1 Ma based on the combined results of all three samples, which individually yield values of 143 ± 6 Ma to 147 ± 2 Ma. The Jeanne d'Arc Formation in Terra Nova K-18 has an estimated maximum depositional age of 145 ± 1 Ma (recalculated from Hutter and Beranek, 2020) based on the combined results of all three samples, which individually yield values of 142 ± 3 Ma to 146 ± 1 Ma.

Table 2
Maximum depositional ages of Bodhrán and Jeanne d'Arc Formation strata calculated with the IsoplotR algorithm of Vermeesch (2021).

Mizzen F-09			
Sample	Depth (m)	Age (Ma)	# of Mesozoic grains
AN20B	3350.80–3354.20	143.4 ± 5.6	1
AN20C	3372.60–3375.00	147.1 ± 1.8	4
AN20D	3384.60–3386.20	145.7 ± 1.8	5
All samples	3350.80–3386.20	146.3 ± 1.3	10
Terra Nova K-18			
Sample	Depth (m)	Age (Ma)	# of Mesozoic grains
17AH01	3265–3271	145.6 ± 0.8	10
17AH03	3306–3311	142.3 ± 2.9	2
17AH02	3317–3323	145.0 ± 1.0	6
All samples	3265–3323	145.2 ± 0.6	18

4.2. Quantitative mineral abundances

Bodhrán formation strata in Mizzen F-09 yield rock-forming (49.88–66.41%; $\overline{X}$ = 56.15%), secondary (13.29–46.25%; $\overline{X}$ = 36.47%), and accessory (0.22–0.98%; $\overline{X}$ = 0.61%) mineral constituents, organic materials (0.20–2.21%; $\overline{X}$ = 0.80), and pore space amounts (0.76–18.79%; $\overline{X}$ = 5.61%) that vary by stratigraphic position (Table 1). The lowermost (3384.60–3386.20 m) and uppermost (3335.00–3337.40 m) samples, which are three very fine-to coarse-grained sandstones from the fluvial and estuarine facies, respectively, generally show the most abundant plagioclase (0.30–0.68%), potassium feldspar (0.86–1.40%), garnet (0.02–0.03%), muscovite (0.27–0.49%), rutile (0.17–0.35%), and staurolite (0.16–0.18%) values in the Bodhrán formation rock suite (Fig. 4; Table 1). These three samples also yield high amounts of secondary minerals such as albite (4.55–13.05%), chlorite (0.14–0.30%), illite (1.66–3.22%), and kaolinite (0.01–1.69%) that are fine-grained clastic and metaclastic rock fragments or alteration phases in igneous rock fragments. Three fine-grained to gravelly fluvial (3372.60–3375.00 m) to tide-modulated fluvial (3345.20–3350.80 m) units that comprise the middle part of the drillcore section have comparably lower amounts of plagioclase (0.16–0.20%), potassium feldspar (0.29–1.02%), accessory minerals like garnet (0.01–0.03%), rutile (0.04–0.07%), and staurolite (0.04–0.07%), and secondary or alteration minerals like albite (1.89–3.73%), chlorite (0.08–0.11%), illite (0.78–2.02%), and kaolinite (0.17–0.67%). Bodhrán formation samples show decreasing porosity (0.76–18.79%) with increasing amounts of calcite cement (2.65–42.18%).

Jeanne d'Arc Formation strata in Terra Nova K-18 yield generally similar rock-forming (61.78–75.91%; $\overline{X}$ = 70.42%) and accessory (0.08–0.14%; $\overline{X}$ = 0.10%) mineral constituents and organic materials (0.14–0.35%; $\overline{X}$ = 0.28); the amount of secondary minerals (2.75–33.44%; $\overline{X}$ = 14.26%) is positively correlated with pore space amounts (4.45–20.88%; $\overline{X}$ = 14.88%) and shows no systematic change with stratigraphic position. Very fine-to coarse-grained sandstone units of the Jeanne d'Arc Formation yield plagioclase (0.03–0.06%), potassium feldspar (0.07–0.09%), garnet (0.01%), muscovite (<0.01–0.06%), rutile (0.01–0.06%), and staurolite (0.01–0.03%) values that are generally an order of magnitude lower than those of the Bodhrán formation.

5. Detrital zircon provenance interpretations

5.1. Mesozoic age populations

Mesozoic detrital zircon grains (ca. 143–161 Ma, <1–3% of each sample) have subrounded to angular morphologies and interpreted to have provenance from Grand Banks rift successions (Table 3). The existence of Jurassic to Cretaceous igneous or pyroclastic rocks that intrude or cover Appalachian basement in the northern Flemish Pass region is uncertain, however, nearby sources may be represented by magnetic anomalies that underlie the Cumberland magnetic belt to the west or Beothuk Knoll to the southeast (e.g., Enachescu, 1987).

Potential Mesozoic sources more distal to Mizzen F-09 require long-distance sediment transport into the northern Flemish Pass basin. Late Jurassic (ca. 146–148 Ma) gabbro intrusions and lampophyre dikes in the Notre Dame Bay region of the north-central Newfoundland

Table 3
Summary of primary and recycled detrital zircon sources for Bodhrán formation strata modified from Hutter and Beranek (2020).

Age populations	Potential primary sources	Potential recycled sources in Atlantic Canada & Iberia
Archean >2500 Ma	Superior, North Atlantic, Nain cratons	Iapetan margin sandstones, Appalachian (peri-Laurentian, Gondwanan-, Baltican) terrane cover assemblages
Proterozoic 2200-2000 Ma	Gondwanan or Baltican cratons	Appalachian terrane cover assemblages, Variscan metasedimentary rocks
2000-930 Ma	Torngat, New Quebec, Trans-Hudson, Grenville and related orogens	Iapetan margin sandstones, Appalachian foreland & strike-slip basins Variscan metasedimentary rocks
720-541 Ma	Peri-Gondwanan or Baltican terranes	Appalachian terrane cover assemblages, Appalachian foreland & strike-slip basins, Variscan metasedimentary rocks
Paleozoic 530-271 Ma	Appalachian-Variscan igneous suites	Appalachian-Variscan foreland & strike-slip basins
Mesozoic 161-143 Ma	North Atlantic rift assemblages	Oxfordian to Tithonian strata, Grand Banks

Appalachians (Peace et al., 2019), ~600 km west-northwest of Mizzen F-09, overlap with the late Tithonian age of the Bodhrán formation. Tithonian to Berriasian and older volcanic centers and associated intrusive complexes are also recognized along the SW Grand Banks fault zone and Collector anomaly (e.g., Pe-Piper et al., 2007; Bowman et al., 2012) ~600 km southwest of Mizzen F-09. These southern igneous systems were likely the sources of Mesozoic detrital zircon grains in Tithonian Jeanne d'Arc Formation strata (Hutter and Beranek, 2020). Along the Iberian conjugate margin, ca. 141–147 Ma alkaline mafic rock units are recognized between the Nazaré and Tagus Valley fault zones in onshore parts of the Lusitanian basin (Grange et al., 2008; Mata et al., 2015) and ca. 140–167 Ma amphibolite units are inferred at Ocean Drilling Program sites 1067 and 1068 (Jagoutz et al., 2007).

5.2. Paleozoic age populations

Early to late Paleozoic detrital zircon grains (ca. 271–530 Ma, 17–22% of each sample) yield age peaks of 278, 354, 375, 393, 432, 452, and 480 Ma and are interpreted to have provenance from Appalachian-Variscan igneous rocks and related sedimentary basins (Table 3) that were exhumed during Mesozoic rifting. Example primary sources in the Newfoundland Appalachians include Ordovician to Devonian rocks generated during the Taconic, Salinic, and Acadian orogenic phases (e.g., Dunning et al., 1990; O'Brien et al., 1996; Valverde-Vaquero et al., 2006; Kellett et al., 2014; van Staal et al., 2021a). Mississippian and younger foreland and strike-slip basin strata yield Paleozoic and older detrital zircon grains (e.g., Murphy and Hamilton, 2000; Force and Barr, 2012) and are potential recycled sources along the Newfoundland and northern Nova Scotia margins. Primary sources in the Variscan belt of Iberia include igneous rocks in the Central Iberian and Ossa-Morena zones (e.g., Valverde-Vaquero and Dunning, 2000; Solá et al., 2008), some of which locally sourced upper Paleozoic and syn-rift Mesozoic strata in Portugal (e.g., Dinis et al., 2016, 2018, 2021; Pereira et al., 2016). Pennsylvanian to early Permian detrital zircon grains indicative of late Variscan granitoids in Iberia are rare, however, mid-Permian (ca. 271–280 Ma) age populations in the Bodhrán formation overlap with rocks generated during Variscan collapse (Fernández-Suárez et al., 2000; Hildenbrand et al., 2021). A direct source from the Iberian massif is not preferred based on evidence for a topographic high to the west of the Lusitanian basin (Berlengas block; e.g., Dinis et al., 2021), but we interpret that Iberian-sourced, upper Paleozoic foreland basin or cover assemblage strata in the Grand Banks region to the west of the Variscan front were exhumed and recycled during Tithonian extension. Cretaceous strata at ODP Site 1276 south of Flemish Cap yield ca. 270–340 Ma white mica derived from upper Paleozoic foreland basin deposits originally sourced from the Iberian Variscides (Hiscott et al., 2008).

5.3. Late to mid-Neoproterozoic age populations

Late to mid-Neoproterozoic detrital zircon grains (ca. 541–720 Ma, 30–58% of each sample) yield a main age peak of 613 Ma and are interpreted to have provenance from peri-Gondwanan or peri-Baltican arc rocks (e.g., van Staal et al., 2021a) and overlapping basins in the North Atlantic region (Table 3). Example primary sources in Atlantic Canada include Ediacaran to Cryogenian arc complexes of Avalonia in onshore parts of the Newfoundland Appalachians and offshore regions such as Flemish Cap (e.g., King et al., 1985; Krogh et al., 1988; O'Brien et al., 1996). Primary sources in Iberia include Ediacaran to Cryogenian igneous rocks that are related to Cadomian tectonic evolution (e.g., Pereira et al., 2008; Henriques et al., 2018). Similar superchrondritic to subchondritic, late to mid-Neoproterozoic detrital zircon grains in Jeanne d'Arc basin syn-rift units were recycled through upper Paleozoic strata (Hutter and Beranek, 2020) and it is likely that analogous sedimentary assemblages fed multi-cycle, ca. 541–720 Ma detrital zircon grains into the northern Flemish Pass basin.

5.4. Early Neoproterozoic to Paleoarchean age populations

Early Neoproterozoic to Paleoarchean detrital zircon grains (ca. 930–3300 Ma; 22–46% of each sample) yield age peaks of 976, 1066, 1163, 1281, 1334, 1395, 1642, 1813, 2080, 2622, and 2728 Ma and are interpreted to have original provenance from Precambrian basement rocks (Table 3); these grains are interpreted as polycyclic and recycled through pre-existing sedimentary rocks into the Bodhrán formation. Early Neoproterozoic to latest Paleoproterozoic (ca. 930–1700 Ma) detrital zircon ages correspond to processes that constructed the Grenville orogen and younger sedimentary systems of eastern Laurentia and Baltica (e.g., Rivers, 1997; Rainbird et al., 2017). Original and recycled sources in Atlantic Canada include basement massifs and overlying Ediacaran to lower Paleozoic continental margin strata in western Newfoundland (e.g., Cawood and Nemchin, 2001). Late to mid-Paleoproterozoic (ca. 1800–2000 Ma) detrital zircon ages correlate with rock units assigned to the Torngat, Trans-Hudson, New Quebec, and related orogens (Hoffman, 1988; Whitmeyer and Karlstrom, 2007). Early Paleoproterozoic (ca. 2000–2200 Ma) detrital zircon grains are minor; these ages are rare in North America and suggest recycled West Gondwana (e.g., Willner et al., 2013) or Baltican (van Staal et al., 2021b) craton sources that were incorporated into Appalachian basement successions. Archean (>2500 Ma) ages correspond to magmatism in the Superior, Nain, and other cratons of Laurentia (e.g., Hoffman, 1988). Early Neoproterozoic to Archean detrital zircon grains with Iberian provenance could have been recycled through Ediacaran to Paleozoic metasedimentary rocks involved in Variscan tectonic evolution (e.g., Braid et al., 2011; Pereira et al., 2012; Rodrigues et al., 2015; Dinis et al., 2018).

6. Sandstone mineralogy and provenance interpretations

6.1. Bodhrán formation

Quantitative SEM-MLA results (Table 1) demonstrate that Bodhrán formation rocks in Mizzen F-09 yield primary igneous (e.g., feldspar), metamorphic (e.g, staurolite), and sedimentary (e.g., recycled quartz) constituents, which are consistent with derivation from Proterozoic to Paleozoic basement complexes and their cover assemblages. Feldspar, clay, and other igneous minerals are probably tied to the same rock sources as the major detrital zircon U–Pb age peaks (e.g., 146, 278–480, 613 Ma) in the Bodhrán formation and therefore have several potential

origins in the Appalachian (e.g., Avalonia) and Variscan (e.g., Central Iberian zone) orogens and Newfoundland-Iberia rift system. Albite and illite occurrences reflect some detrital input from altered feldspar (cf., Xiong et al., 2016), and these and other clay species, including chlorite and kaolinite, are similarly consistent with the inferred composition of mudrock clasts and igneous lithics with seafloor or hydrothermal alteration-related minerals. For example, ca. 570–625 Ma volcanic units that comprise the exposed basement in eastern Newfoundland, which are interpreted to be analogous to those that underlie Flemish Cap and other highlands adjacent to the Mizzen discovery, show evidence for the hydrothermal alteration of glass and primary igneous minerals (e.g., O'Brien et al., 2001; Arbiol et al., 2021). On the other hand, it is also probable that rift-related, Tithonian igneous sources in the Mizzen discovery region shed some altered and fresh feldspar grains and altered igneous rock fragments into the Flemish Pass basin during Bodhrán formation deposition (cf., Pe-Piper et al., 2007). Appalachian-Variscan rock successions were variably affected by greenschist facies metamorphism (e.g., O'Brien et al., 1996; Bento dos Santos et al., 2021), and may have recycled some albite, chlorite, and possibly muscovite into the Flemish Pass basin.

Fluvial and estuarine lithofacies that comprise the lower (3384.60–3386.20 m) and uppermost (3335.00–3337.40 m) sections of Mizzen F-09 drillcore, respectively, yield the greatest garnet, staurolite, muscovite, rutile, and titanite values in the Bodhrán formation sample suite. The lowermost fluvial strata also have a mid-Permian (ca. 271–280 Ma) detrital zircon population that corresponds in age with igneous rocks generated during Variscan collapse (e.g., Fernández--Suárez et al., 2000; Hildenbrand et al., 2021). We therefore interpret that some metamorphic minerals and metamorphic lithic fragments in the Bodhrán formation similarly have ultimate provenance from the Variscan orogen. Upper Paleozoic cover assemblages in the Grand Banks to the west of the Variscan front contained metamorphic detritus (e.g., Hiscott et al., 2008) and the recycling of such rocks into the Flemish Pass and other rift basins during Tithonian extensional deformation is likely.

Secondary minerals in Bodhrán formation strata include ankerite, calcite, dolomite, and pyrite that are the result of diagenetic processes during burial. The dissolution-cementation histories of Bodhrán formation strata are complex and likely controlled the reservoir quality of Tithonian sandstone units in the Mizzen discovery area (Xiong et al., 2016). The SEM-MLA results in Table 1 correspondingly show a correlation between porosity and carbonate cement modal abundances in the Bodhrán formation. For example, fluvial rocks from 3384.60 to 3386.20 m yield low porosity (0.76%, 2.41%) and high carbonate (34.98%, 36.59%) abundances, whereas tide-modulated fluvial strata from 3350.80 to 3354.20 m yield high porosity (18.79%) and low carbonate (5.41%) abundances.

6.2. Jeanne d'Arc Formation

Fluvial lithofacies of the Jeanne d'Arc Formation contain detrital mineral grains and lithic fragments that indicate similar sources for Tithonian syn-rift units in the Terra Nova oil field. Quantitative SEM-MLA results (Table 1) show that Jeanne d'Arc Formation rocks in Terra Nova K-18 generally have lower abundances of primary igneous (e.g., feldspar) and metamorphic (e.g, staurolite) minerals and higher abundances of sedimentary (e.g., recycled quartz) minerals than coeval strata in the northern Flemish Pass basin. These results support the conclusions of Hutter and Beranek (2020) and argue for Tithonian braided fluvial units to have provenance from quartz-dominated, upper Paleozoic strata that overlie Avalonia-Meguma basement rocks in the Avalon Uplift region and Jurassic igneous systems along the SW Grand Banks fault zone and Collector anomaly.

7. Discussion

7.1. Tithonian depositional age for the Bodhrán formation and evidence of Jurassic syn-rift magmatism in the Grand Banks stratigraphic record

Late Jurassic depositional ages for the Bodhrán formation were previously inferred by microfossil assemblages in Mizzen F-09 drillcore from 3330 to 3760 m-depth (Ainsworth et al., 2015). New detrital zircon U–Pb results for three rock samples from 3350 to 3386 m-depth confirm late Tithonian (146 ± 1 Ma) maximum depositional ages for the Ti-3 sandstone interval (Table 2). These new results furthermore show that Tithonian detrital zircon grains are predictable time-stratigraphic markers for syn-rift, oil-bearing units of the Bodhrán formation and are potentially useful tools for future hydrocarbon exploration activities. For example, drill cuttings of inferred Late Jurassic age from Mizzen L-11, Mizzen O-16, and Baccalieu I-78 in the northern Flemish Pass basin yield ca. 140–150 Ma detrital zircon grains (McDonough et al., 2011; Lowe et al., 2011) and are prospective correlatives of Bodhrán formation reservoir units in Mizzen F-09. Maximum depositional age estimates for syn-rift, Jeanne d'Arc Formation strata in the Terra Nova K-18 well, Jeanne d'Arc basin, overlap within error of the Bodhrán formation at 145 ± 1 Ma (Table 2) and demonstrate the prolific generation of high-quality reservoir units in Grand Banks rift basins during the late Tithonian.

Offshore scientific drilling and onshore bedrock studies have generally recognized Cretaceous igneous, pyroclastic, and epiclastic rocks along the Newfoundland-SE Grand Banks margin (e.g., Pe-Piper et al., 1994; Hart and Blusztajn, 2006; Jagoutz et al., 2007; Bowman et al., 2012). More recently, preliminary zircon U–Pb results have shown evidence for older, Late Jurassic (ca. 146–148 Ma) rift-related magmatism in north-central Newfoundland (Peace et al., 2019) that overlaps in error with late Tithonian detrital zircon grains in syn-rift, Flemish Pass (this study) and southern Jeanne d'Arc (Hutter and Beranek, 2020) basin strata. Moreover, the detrital zircon records of Mizzen F-09 and Terra Nova oil field strata provide compelling evidence for a nearly continuous, Kimmeridgian to Tithonian (ca. 155-145 Ma; 71 grains) episode of magmatism and there are single-grain ages that also point towards an Oxfordian (ca. 160 Ma) event in the Grand Banks. The latter show that late Middle to early Late Jurassic rifting was accompanied by regional volcanism, which has not been recognized previously (e.g., Sinclair, 1988; Manatschal, 2004). The Hf isotope compositions of Jurassic detrital zircon grains in Tithonian strata of the Grand Banks are consistently chondritic to superchondritic (this study; Hutter and Beranek, 2020) and may reflect repeated partial melting of lithospheric mantle (e.g., Pe-Piper et al., 2007) along master detachment faults or transfer zone systems during transtension (e.g., Vaughn and Scarrow, 2003).

7.2. Implications for the timing and extent of magma-poor rift processes in the Newfoundland-Iberia rift system

Magma-poor rift margin systems are divided into architectural segments or morphogeological belts that result from depth-dependent extensional processes and seaward migration of strain towards the future plate margin (e.g., Péron-Pinvidic et al., 2013). The Newfoundland margin was defined by Huismans and Beaumont (2011, 2014) as a Type I end-member margin that included the development of major basin-forming faults in the proximal domain, a narrow transition or necking region with abrupt thinning of continental crust, exhumation of serpentinized continental mantle in the distal domain, and crustal breakup prior to mantle lithosphere breakup. Mesozoic rift basin deposits, which have been tapped by industry wells in the Grand Banks, are the stratigraphic archives of tectonic and thermal subsidence events and can help reconstruct the timing and significance of magma-poor rift evolution. Most models for Newfoundland-Iberia evolution involve superposed Late Triassic to Early Jurassic, Middle to Late Jurassic, and

Early to mid-Cretaceous rift episodes that resulted in tectonic subsidence and filling of proximal domain basins (e.g., Hiscott et al., 1990; Alves et al., 2006; Péron-Pinvidic and Manatschal, 2009; Welsink and Tankard, 2012), some of which overlapped with Late Jurassic to Early Cretaceous crustal thinning and mantle exhumation. Alves and Cunha (2018) concluded that earliest Cretaceous (Berriasian) crustal rupture and mid-Cretaceous (Aptian) lithospheric mantle rupture along the Iberian margin were followed by the deposition of Lower to mid-Cretaceous and mid-to Upper Cretaceous breakup sequences that migrated northwards and oceanwards, respectively. Soares et al. (2012) similarly interpreted a mid-to Upper Cretaceous breakup sequence along the distal Newfoundland margin after Aptian-Albian breakup.

Late Tithonian development of the northern Flemish Pass basin was accommodated by extension-related tectonic exhumation, forced regression, erosion of adjacent Paleozoic to Mesozoic highlands, and deposition of terrestrial to marginal marine strata analogous to other Late Jurassic fluvial systems in Grand Banks (e.g., Hiscott et al., 1990; Cody et al., 2012; Hutter and Beranek, 2020). A key finding of our study is the recognition of syn-rift, late Tithonian magmatism in the northern Flemish Pass basin region that overlaps with the timing of extension-related igneous events in the north-central Newfoundland Appalachians (Peace et al., 2019), SW Grand Banks fault zone region (Hutter and Beranek, 2020), north-central Lusitanian basin of Portugal (Grange et al., 2008; Mata et al., 2015), and distal Iberian margin (Jagoutz et al., 2007). Although some late Tithonian magmatism was structurally-controlled along transfer zones or inherited Appalachian-Variscan lineaments (e.g., Bowman et al., 2012; Pereira et al., 2017), the evidence supports that igneous activity occurred over a wide geographic area and was the result of plate-scale processes in the rift system. For example, the timing of this widespread magmatism was coincident with tectonic scenarios that feature the Tithonian transition from decoupled to coupled deformation and onset of necking processes along the future Newfoundland margin (e.g., Pérez-Gussinyé and Reston, 2001; Sutra et al., 2013), which allowed for some normal faults to propagate into the lithospheric mantle. Along the SW Iberian margin, Tithonian crustal breakup in the southern parts of the rift system is inferred by the M20 magnetic anomaly in the Tagus Abyssal Plain (Srivastava et al., 2000; Alves and Cunha, 2018) although these Late Jurassic features may instead reflect intrusions into thinned crust or magnetization of serpentinite (e.g., Tucholke et al., 2007). If the model of Srivastava et al. (2000) is correct, the syn-rift, forced-regressive intervals of the Flemish Pass (Bodhrán formation) and Jeanne d'Arc (Jeanne d'Arc Formation) basins may record a northern stratigraphic response to SW Iberian continental breakup. A complicating factor in understanding Flemish Pass basin evolution is the proposed clockwise rotation and dextral displacement of Flemish Cap during the Late Jurassic to Cretaceous (e.g., Sibuet et al., 2007; Welford et al., 2010); these interpretations may require oblique-slip extensional deformation (e.g., McDonough et al., 2011; Nirrengarten et al., 2018) in the Flemish Pass basin region that was coincident with stretching in other parts of the proximal domain and hyperextension in the necking domain.

7.3. Late Jurassic stratigraphic connections and SE Grand Banks-Iberia paleogeography

The Late Jurassic paleogeography of the Grand Banks-Iberia rift system is a matter of debate, including the Flemish Pass basin where there are competing models for Bodhrán formation provenance and regional source-to-sink histories (e.g., Lowe et al., 2011; Cody et al., 2012). Some of the critical problems along the Newfoundland margin include the unknown locations of syn-rift, volcanic-intrusive centers that were sampled by Tithonian fluvial systems and potential Late Jurassic sediment contributions from the Iberian massif or Iberian-derived, Variscan foreland basin successions (e.g., Hiscott et al., 2008; McDonough et al., 2011).

Hutter and Beranek (2020) proposed that Bodhrán formation rocks in the Mizzen discovery were potentially correlative with Jeanne d'Arc Formation strata in the Terra Nova oil field (Fig. 6A and B), and based on available detrital zircon U–Pb-Hf isotope provenance constraints, hypothesized southern sources (e.g., Avalon Uplift) for some Tithonian fluvial units in the Flemish Pass basin. Maximum depositional age estimates confirm their time-equivalence within error, but our new quantitative mineral and detrital zircon U–Pb-Hf isotope results are not consistent with stratigraphic connections between southern Jeanne d'Arc and northern Flemish Pass basin rocks and more likely indicate coeval sedimentation in unconnected depocenters. Jeanne d'Arc Formation strata are quartz-dominated and generally lack chemically unstable minerals (e.g., feldspar, garnet, muscovite, rutile, staurolite) that characterize Tithonian sandstone units in Mizzen F-09. Jeanne d'Arc Formation strata were mostly derived from upper Paleozoic successions in the Maritimes basin system of Atlantic Canada (Hutter and Beranek, 2020), and the new mineralogical results from Terra Nova K-18 drillcore show that such upper Paleozoic sources in the Avalon Uplift area were depleted in chemically unstable minerals or that such grains were destroyed during Tithonian fluvial transport and alluvial storage.

Statistical assessments (Cross-correlation, Likeness, and Similarity coefficients of PDPs, Kolmogorov-Smirnov and Kuiper tests) in Appendix B (Table S2) are briefly summarized here to evaluate the similarities between Grand Banks detrital zircon samples. In general, we follow the statistical interpretations of Saylor and Sundell (2016) and favor Cross-correlation coefficients (R^2 values range from 0 to 1 with a cross-plot value of 1 indicating identical age peaks) because they are sensitive to the presence or absence, relative magnitude, and shape of age peaks in PDPs. The three Bodhrán formation samples yield Cross-correlation coefficients of 0.68–0.72 ($\overline{X} = 0.70$) and based on the number of grains analyzed (see Saylor and Sundell, 2016), we do not reject the hypothesis that these fluvial to tide-modulated fluvial strata were drawn from the same source. Cross-correlation coefficients between Bodhrán formation rocks and Jeanne d'Arc Formation strata in Terra Nova K-18 (0.18–0.75, $\overline{X} = 0.40$), C-09 (0.23–0.61, $\overline{X} = 0.43$), and E−79 (0.16–0.64, $\overline{X} = 0.38$) are lower than those observed for intra-Mizzen F-09 comparisons and based on our quantitative mineral results we conclude these statistical data indicate derivation from different populations. Jeanne d'Arc Formation strata at Terra Nova were derived from similar Avalon Uplift sources (Hutter and Beranek, 2020) and intra-well comparisons show similar Cross-correlation coefficients in K-18 (0.47–0.61, $\overline{X} = 0.55$), C-09 (0.54–0.58, $\overline{X} = 0.56$), and E−79

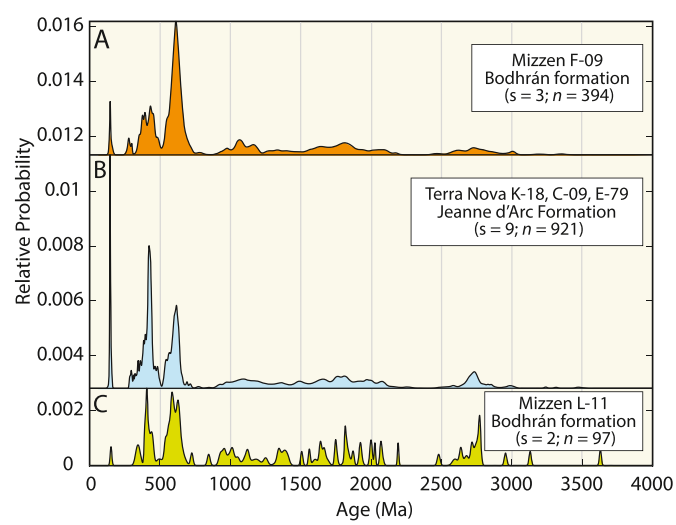

Fig. 6. Detrital zircon U–Pb ages for late Tithonian strata in (A) Mizzen F-09 (this study), (B) Terra Nova K-18, C-09, and E−79 (Hutter and Beranek, 2020), and (C) Mizzen L-11 (compiled from Lowe et al. (2011). s = detrital zircon samples, n = number of detrital zircon grains.

(0.31–0.63, $\overline{X} = 0.49$). The Mizzen F-09 and Terra Nova K-18 drillcore samples were both selected from relatively thin (<100 m) stratigraphic intervals without major depositional interruptions and therefore these statistical outcomes could reflect the poor mixing of fluvial systems (e.g., DeGraaff-Surpless et al., 2003) that drained geographically different, but geologically similar, sediment source regions. Multi-Dimensional Scaling (MDS) results of Tithonian strata generally support the Cross-correlation coefficients and demonstrate that the lowermost fluvial sample in Mizzen F-09 (AN20D) is dissimilar to most Jeanne d'Arc Formation rocks in the Terra Nova oil field, and has some differences with respect to overlying Bodhrán formation strata (Fig. 7). Apparent statistical differences likely result from the lowermost fluvial sample having the ca. 271–280 Ma age grouping that is generally missing from overlying strata and the greatest percentage of mid-to late Neoproterozoic detrital zircon grains (58%) in the Mizzen F-09 suite. The upper fluvial and tide-modulated fluvial samples in Mizzen F-09 correspondingly cluster with each other and single samples of Jeanne d'Arc Formation strata in wells K-18, C-09, and E−79 (Fig. 7).

Lowe et al. (2011) proposed that Upper Jurassic strata in Mizzen L-11 (Fig. 6C) were mostly derived from Neoproterozoic and younger basement and cover assemblages and interpreted 400–500 km of east-directed sediment transport from the Newfoundland Appalachians to the northern Flemish Pass basin; some first-cycle Paleoproterozoic and Neoarchean detrital zircon grains were also interpreted in Mizzen L-11, which would require craton sources from southern Greenland or Labrador as crystalline basement rocks of these ages are lacking in the Appalachian orogen. Lowe et al. (2011) further concluded that Avalonian and Variscan basement rock units from Flemish Cap and the Iberian massif, respectively, were not primary sources for their Mizzen L-11 samples. The results of Lowe et al. (2011) were filtered to match our zircon U–Pb data handling protocols for the Mizzen F-09 and Terra Nova oil field wells and the low-n values of the two samples (recalculated at $n = 43$ and 54) likely produce some statistical limitations. Proposed Upper Jurassic stratigraphic correlations between Mizzen L-11 and Mizzen F-09 (Cody et al., 2012), located ~15 km apart, are generally supported by the statistical assessments, including Cross-correlation coefficients of

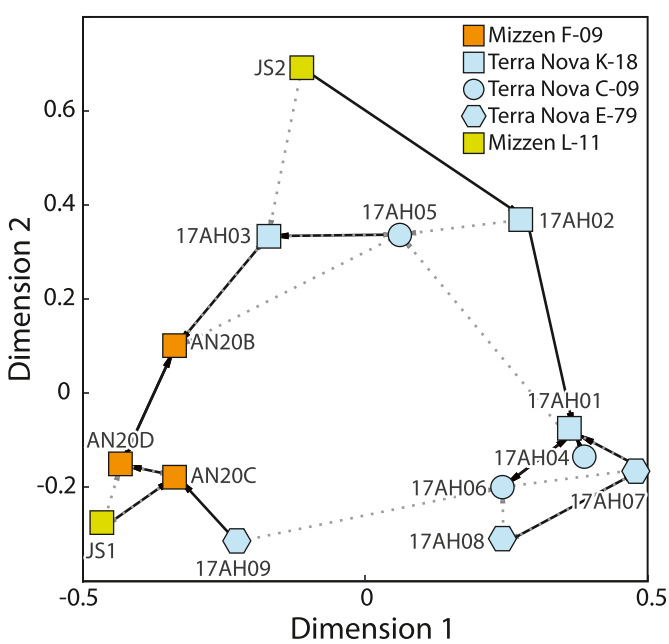

Fig. 7. 2D multidimensional scaling plot of detrital zircon U–Pb age distributions from Mizzen F-09 (this study), Terra Nova K-18, C-09, and E−79 (Hutter and Beranek, 2020), and Mizzen L-11 (Lowe et al., 2011). The plot uses the Cross-correlation coefficient to calculate dissimilarity. The corresponding Shepard plot is available in the Appendix (Table S2).

0.51–0.65 between the Mizzen F-09 samples and Jurassic Sandstone 1 of Lowe et al. (2011). MDS results correspondingly show that Jurassic Sandstone 1 of Lowe et al. (2011) has some similarities with fluvial rocks in Mizzen F-09 (AN20C, AN20D), whereas Jurassic Sandstone 2 of Lowe et al. (2011) broadly clusters with Jeanne d'Arc Formation fluvial strata in Terra Nova K-18 and C-09 (Fig. 7). We prefer a scenario with Mizzen L-11 and Mizzen F-09 strata being correlative, but neither of those Upper Jurassic sections have continuity with Tithonian rocks of the southern Jeanne d'Arc basin or direct connections with the Newfoundland Appalachians to the west. Future detrital zircon U–Pb-Hf isotope studies of Mizzen L-11 cuttings are warranted and we predict that high-n investigations will yield Late Jurassic to Neoarchean age populations analogous to those in Mizzen F-09, including ca. 271–280 Ma grains of Iberian provenance.

Cody et al. (2012) and Beicip-Franlab (2015) proposed Late Jurassic paleogeographic reconstructions for the Flemish Pass basin region based on industry well and geophysical data. Potential Late Jurassic strike-slip deformation and rotation of Flemish Cap are not explicitly defined in these two reconstructions and therefore drainage vectors quoted below are unrestored, modern cardinal directions. Cody et al. (2012) interpreted Bodhrán formation strata in the Mizzen discovery to comprise parts of a southwest-directed, axial fluvial system that drained a rift graben near the northwestern flank of Flemish Cap, whereas Beicip-Franlab (2015) predicted that Mizzen discovery strata were part of a west-to northwest-directed, fluvial-deltaic system with potential headwaters in Flemish Cap, Beothuk Knoll, and other highlands to the south-southeast. Our new provenance results do not provide a unique solution to this debate, but based on the potential for Late Jurassic igneous rocks at Beothuk Knoll (e.g., Enachescu, 1987) and interpreted southeast-to-northwest transition from shallow-to deep-water facies in the Mizzen discovery area (Beicip-Franlab, 2015), we hypothesize that the latter model is most consistent with the detrital zircon U–Pb-Hf isotope signatures and mineral constituents of Bodhrán formation strata (Fig. 8). Late Jurassic igneous rock sources in the Cumberland magnetic belt to the west of the Mizzen discovery are also permissible and could point to other local contributions. Seismic and ocean drilling studies have observed a lack of Paleozoic cover assemblages on Beothuk Knoll and Flemish Cap (e.g., King et al., 1985; Van Avendonk et al., 2006) and we interpret that these missing strata were stripped off during Mesozoic exhumation and shed into the adjacent Flemish Pass basin. Some of these sources included upper Paleozoic successions that were repositories of garnet, muscovite, rutile, staurolite and other chemically unstable minerals (e.g., Hiscott et al., 2008) originally sourced from metasedimentary and metaigneous rocks in the Variscan orogen of Iberia (e.g., Ribeiro et al., 1990; Bento dos Santos et al., 2021).

Primary basement sources exposed along the Iberian conjugate margin are not preferred for Mizzen discovery strata, but they did deliver Variscan-related sediment to the Lusitanian basin prior to the Tithonian. For example, Lower to Middle Jurassic marine to marginal-marine strata in the southwestern Lusitanian basin yield west-derived, late Paleozoic (ca. 270–330 Ma) and Ediacaran (ca. 550–640 Ma) detrital zircon grains and chlorite, garnet, staurolite, and other minerals originally from Variscan and enclosing Cadomian basement rocks of the Berlengas block, respectively (Fig. 8; Dinis et al., 2021). West-derived Cabo Carvoeiro Formation (Toarcian) and Alcobaça Formation (Kimmeridgian) units of the Lusitanian basin do not have provenance ties with Tithonian strata along the Newfoundland margin and yield low Cross-correlation coefficients (0.00–0.03, $\overline{X} = 0.01$) when compared with Bodhrán and Jeanne d'Arc Formation samples. Notably, one sample of the Abadia Formation (Kimmeridgian) that regionally underlies syn-rift, Tithonian fluvial units of the Lourinhã Formation gives higher Cross-correlation values (0.08–0.82, $\overline{X} = 0.29$) when compared with Upper Jurassic strata along the Newfoundland margin, especially for Bodhrán formation rocks in Mizzen F-09 (0.49–0.82, $\overline{X} = 0.61$). The strongest statistical comparisons for the Abadia Formation sample are

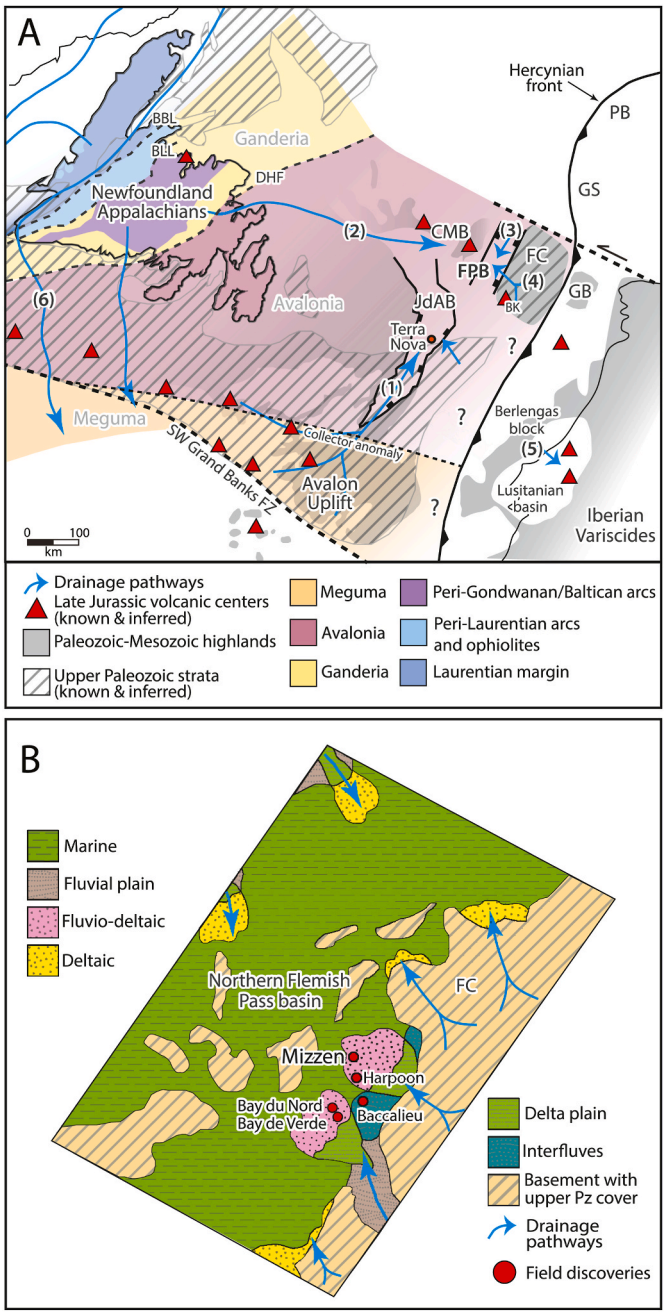

Fig. 8. Cartoon Late Jurassic paleogeography of the Grand Banks region. (A) Published drainage models for sediment flux into the Flemish Pass basin: (1) southern sources from the Avalon Uplift (Hutter and Beranek, 2020); (2) western sources from Newfoundland Appalachians (Lowe et al., 2011); (3) northern sources from Flemish Cap (Cody et al., 2012); and (4) eastern-southeastern sources from Flemish Cap and Beothuk Knoll region (Beicip-Franlab, 2015). Continent-scale drainage models (5) and (6) are based on Piper et al. (2012) and Dinis et al. (2021) for the Scotian and Lusitanian basins, respectively. Locations of Late Jurassic igneous rocks compiled from Jagoutz et al. (2007), Bowman et al. (2012) and Mata et al. (2015). BBL –Baie Verte-Brompton Line, BK – Beothuk Knoll, BLL – Beothuk Lake Line (former Red Indian Line), CMB – Cumberland magnetic belt, DHF – Dover-Hermitage Bay fault, FC – Flemish Cap, FPB – Flemish Pass basin, FZ – fault zone, GB – Galicia Bank, GS – Goban Spur, JdAB – Jeanne d'Arc basin, PB – Porcupine Bank, SW – Southwest. (B) Proposed Late Jurassic paleogeography of the Mizzen discovery area modified from Beicip-Franlab (2015). FC – Flemish Cap. (For interpretation of the references to colour in this figure legend, the reader is referred to the Web version of this article.)

the lowermost fluvial strata in Mizzen F-09 (0.82) that yield the greatest abundance of metamorphic detritus and ca. 271–280 Ma detrital zircon grains with Variscan provenance. Given the available geological constraints, we propose that these Abadia Formation data represent a proxy detrital mineral provenance signature for upper Paleozoic assemblages to the west of the Variscan front that were recycled into the northern Flemish Pass basin during Late Jurassic extension. Detrital zircon U–Pb-Hf isotope and related provenance studies of Tithonian strata in the Lusitanian basin (Lourinhã Formation and equivalents) are required to further test the Late Jurassic paleogeography of the Newfoundland-Iberia margins.

8. Conclusions

Detrital mineral studies of Bodhrán formation strata provide new constraints on the timing of syn-rift subsidence in the northern Flemish Pass basin and the significance of Mizzen discovery reservoir units to regional tectonics and paleogeography. Bodhrán formation fluvial to tide-modulated fluvial strata were deposited during a late Tithonian (ca. 146 Ma) rift episode that was coincident with the reactivation of existing proximal domain faults, onset of necking processes in the Grand Banks, generation of extension-related igneous rocks across the width of the Newfoundland-Iberia rift system, and potentially the timing of crustal breakup along SW Iberia. New detrital zircon U–Pb ages confirm that Ti-3 reservoir units in Mizzen F-09 are the same depositional age within error as producing sandstones in the Terra Nova oil field, Jeanne d'Arc basin, and demonstrate the remarkable prospectivity of Tithonian terrestrial and marginal-marine strata in the Grand Banks. Late Jurassic detrital zircon grains in Bodhrán formation rocks were sourced from igneous complexes at Beothuk Knoll or other nearby uplifts, whereas late Paleozoic to Paleoarchean detrital zircon populations and unstable mineral constituents (feldspar, garnet, muscovite, rutile, staurolite) have provenance from Appalachian-Variscan basement and cover units, including upper Paleozoic strata ultimately sourced from the Variscan orogen of Iberia. Siliciclastic sediment that fed the northern Flemish Pass basin was probably sourced from now-missing cover assemblages stripped off Flemish Cap, Beothuk Knoll, and nearby highs. Late Jurassic paleogeographic models that predict Bodhrán formation strata as part of a west-to northwest-directed fluvial-deltaic system with headwaters to the south-southeast are consistent the detrital zircon and quantitative mineral results.

Declaration of competing interest

The authors declare that they have no known competing financial interests or personal relationships that could have appeared to influence the work reported in this paper.

Data availability

Data will be made available on request.

Acknowledgements

Luke Beranek acknowledges funding support from the National Science and Engineering Council of Canada (NSERC). John Hanchar, Wanda Aylward, Rebecca Lam, and Markus Wälle aided detrital zircon studies at Memorial University of Newfoundland. David Mills at the Canada- Newfoundland and Labrador Offshore Petroleum Board Core Storage and Research Centre facilitated core sampling. Feedback on this project from Steve Piercey, Mike Babechuk, and Mike McDonough is appreciated. Two anonymous reviewers provided constructive comments that improved this manuscript.

Appendix A. Supplementary data

Supplementary data to this article can be found online at https://doi.org/10.1016/j.marpetgeo.2022.105960.

References

Ainsworth, N.R., Riley, L.A., Haynes, S., McDonough, M., Stacey, E., 2015. A Late Jurassic, Tithonian to Early Eocene, Ypresian, stratigraphic framework for the Mizzen F-09, L-11, and O-16 exploration wells, Flemish Pass basin, offshore Newfoundland: Abstracts of the CSPG/ CSEG/CWLS GeoConvention 2015 4. Calgary, Canada, May 4–8, 2015.

Alves, T.M., Cunha, T.A., 2018. A phase of transient subsidence, sediment bypass and deposition of regressive–transgressive cycles during the breakup of Iberia and Newfoundland. Earth Planet Sci. Lett. 484, 168–183. https://doi.org/10.1016/j.epsl.2017.11.054.

Alves, T.M., Moita, C., Sandnes, F., Cunha, T., Monteiro, J.H., Pinheiro, L.M., 2006. Mesozoic-Cenozoic evolution of North Atlantic continental-slope basins: the Peniche basin, western Iberian margin. American Association of Petroleum Geologists 90, 31–60. https://doi.org/10.1306/08110504138.

Alves, T.M., Moita, C., Cunha, T., Ullnaess, M., Myklebust, R., Monteiro, J.H., Manuppella, G., 2009. Diachronous evolution of Late Jurassic-Cretaceous continental rifting in the northeast Atlantic (west Iberian margin). Tectonics 28. https://doi.org/10.1029/2008TC002337.

Arbiol, C., Layne, G.D., Zanoni, G., Šegvić, B., 2021. Characteristics and genesis of phyllosilicate hydrothermal assemblages from Neoproterozoic epithermal Au-Ag mineralization of the Avalon Zone of Newfoundland, Canada. Appl. Clay Sci. 202 https://doi.org/10.1016/j.clay.2020.105960.

Beicip-Franlab, 2015. Offshore Newfoundland & Labrador Resource Assessment, Flemish PassArea NL15-01EN. https://exploration.nalcorenergy.com/wp-content/uploads/2016/09/Atlas_Public_Final_2015-09-30.pdf. (Accessed October 2022).

Bento dos Santos, T., Rodrigues, J.F., Castro, P., Cotrim, B., Pereira, I., Ferreira, J.A., Meireles, C., Ferreira, N., Ferreira, P., Ribeiro, A., Guimarães, F., 2021. Exhumation of an anatectic complex by channel flow and extrusion tectonics: structural and metamorphic evidence from the Porto-Viseu metamorphic belt, Central Iberian Zone. Int. J. Earth Sci. 110, 2179–2201. https://doi.org/10.1007/s00531-021-02067-z.

Beranek, L.P., 2017. A magma-poor rift model for the Cordilleran margin of western North America. Geol. 45, 115–118. https://doi.org/10.1130/G39265.1.

Beranek, L.P., Gee, D.G., Fisher, C.M., 2020. Detrital zircon U-Pb-Hf isotope signatures of Old Red Sandstone strata constrain the Silurian to Devonian paleogeography, tectonics, and crustal evolution of the Svalbard Caledonides. Geol. Soc. Am. Bull. 132, 1987–2003. https://doi.org/10.1130/B35318.1.

Black, L.P., Kamo, S.L., Allen, C.M., Davis, D.W., Aleinikoff, J.N., Valley, J.W., Mundil, R., Campbell, I.H., Korsch, R.J., Williams, I.S., Foudoulis, C., 2004. Improved $^{206}Pb/^{238}U$ microprobe geochronology by the monitoring of a trace-element-related matrix effect; SHRIMP, ID-TIMS, ELA-ICP-MS and oxygen isotope documentation for a series of zircon standards. Chem. Geol. 205, 115–140. https://doi.org/10.1016/j.chemgeo.2004.01.003.

Boillot, G., Grimaud, S., Mauffret, A., Mougenot, D., Kornprobst, J., Mergoil-Daniel, J., Torrent, G., 1980. Ocean-Continent boundary off the Iberian margin: a serpentinite diapir west of the Galicia Bank. Earth Planet Sci. Lett. 48, 23–34. https://doi.org/10.1016/0012-821X(80)90166-1.

Bouvier, A., Vervoort, J.D., Patchett, P.J., 2008. The Lu-Hf and Sm-Nd isotopic composition of CHUR: Constraints from unequilibrated chondrites and implications for the bulk composition of terrestrial planets. Earth Planet Sci. Lett. 273, 48–57. https://doi.org/10.1016/j.epsl.2008.06.010.

Bowman, S.J., Pe-Piper, G., Piper, D.J.W., Fensome, R.A., King, E.L., 2012. Early Cretaceous volcanism in the Scotian basin. Can. J. Earth Sci. 49, 1523–1539. https://doi.org/10.1139/e2012-063.

Braid, J.A., Murphy, J.B., Quesada, C., Mortensen, J.K., 2011. Tectonic escape of a crustal fragment during closure of the Rheic Ocean: U-Pb detrital zircon data from the late Paleozoic Pulo do Lobo and South Portuguese zones, southern Iberia. J. Geol. Soc. 168, 383–392. https://doi.org/10.1144/0016-76492010-104.

Bronner, A., Sauter, D., Manatschal, G., Peron-Pinvidic, G., Munschy, M., 2011. Magmatic breakup as an explanation for magnetic anomalies at magma-poor rifted margins. Nat. Geosci. 4, 549–553. https://doi.org/10.1038/ngeo1201.

C-NLOPB, 2012. Mizzen F-09 Petrographic Study – Rotary Sidewall and Conventional Core Plugs. https://home-cnlopb.hub.arcgis.com/pages/mizzen-f-09. accessed September 2022.

Cawood, P.A., Nemchin, A.A., 2001. Paleogeographic development of the east Laurentian margin: constraints from U-Pb dating of detrital zircons in the Newfoundland Appalachians. Geol. Soc. Am. Bull. 113, 1234–1246. https://doi.org/10.1130/0016-7606(2001)113<1234:PDOTEL>2.0.CO;2.

Cawood, A.J., Ferrill, D.A., Morris, A.P., Norris, D., McCallum, D., Gillis, E., Smart, K.J., 2021a. Tectonostratigraphic evolution of the Orphan basin and Flemish Pass region – Part 1: results from coupled kinematic restoration and crustal area balancing. Mar. Petrol. Geol. 128, 105042 https://doi.org/10.1016/j.marpetgeo.2021.105042.

Cawood, A.J., Ferrill, D.A., Morris, A.P., Norris, D., McCallum, D., Gillis, E., Smart, K.J., 2021b. Tectonostratigraphic evolution of the Orphan basin and Flemish Pass region – Part 2: regional structural development and lateral variations in rifting style. Mar. Petrol. Geol. 133, 105219 https://doi.org/10.1016/j.marpetgeo.2021.105219.

Cody, J., Hunter, D., Schwartz, S., Marshall, J., Haynes, S., Gruschwitz, K., McDonough, M., 2012. A Late Jurassic play fairway beyond the Jeanne d'Arc basin: new insights for a petroleum system in the northern Flemish Pass basin. In: Rosen, N. C., Weimer, P., Coutes de Anjos, S.M., et al. (Eds.), New Understanding of the Petroleum Systems of Continental Margins of the World, vol. 32. SEPM Gulf Coast Section Publication, pp. 599–608. https://doi.org/10.5724/gcs.12.32.0598.

Coffin, M.F., Eldholm, O., 1994. Large igneous provinces: crustal structure, dimensions, and external consequences. Rev. Geophys. 32, 1–36. https://doi.org/10.1029/93RG02508.

Cohen, K.M., Finney, S.C., Gibbard, P.L., Fan, J.-X., 2013. The ICS international chronostratigraphic chart. Episodes 36, 99–204 (updated). http://www.stratigraphy.org/ICSchart/ChronostratChart2022-02.pdf.

Deemer, S., Hall, J., Solvason, K., Lau, K.W.H., Louden, K., Srivastava, S., Sibuet, J.-C., 2009. Structure and development of the southeast Newfoundland continental passive margin: derived from SCREECH Transect 3. Geophys. J. Int. 178, 1004–1020. https://doi.org/10.1111/j.1365-246X.2009.04162.x.

DeGraaff-Surpless, K., Mahoney, J.B., Wooden, J.L., McWilliams, M.O., 2003. Lithofacies control in detrital zircon provenance studies: insights from the Cretaceous Methow basin, southern Canadian Cordillera. Geol. Soc. Am. Bull. 115, 899–915. https://doi.org/10.1130/B25267.1.

DeSilva, N.R., 1999. Sedimentary basins and petroleum systems offshore Newfoundland and Labrador. In: Fleet, A.J., Boldy, S.A.R. (Eds.), Petroleum Geology of Northwest Europe, vol. 5. Geological Society of London, Petroleum Geology Conference Series, pp. 501–515. https://doi.org/10.1144/0050501.

Dinis, P.A., Dinis, J., Tassinari, C., Carter, A., Callapez, P., Morais, M., 2016. Detrital zircon geochronology of the Cretaceous succession from the Iberian Atlantic Margin: palaeogeographic implications. Int. J. Earth Sci. 105, 727–745. https://doi.org/10.1007/s00531-015-1221-z.

Dinis, P.A., Fernandes, P., Jorge, R.C.G.S., Rodrigues, B., Chew, D.M., Tassinari, C.G., 2018. The transition from Pangea amalgamation to fragmentation: constraints from detrital zircon geochronology on West Iberia paleogeography and sediment sources. Sediment. Geol. 375, 172–187. https://doi.org/10.1016/j.sedgeo.2017.09.015.

Dinis, P.A., Vermeesch, P., Duarte, L.V., Cunha, P.P., Barbarano, M., Garzanti, E., 2021. The Variscan basement in the western shoulder of the Lusitanian Basin (West Iberian Margin): insights from detrital-zircon geochronology of Jurassic strata. J. Iber. Geol. 47 https://doi.org/10.1007/s41513-021-00177-w, 865-696.

Dunning, G.R., O'Brien, S.J., Colman-Sadd, S.P., Blackwood, R.F., Dickson, W.L., O'Neill, P.P., Krogh, T.E., 1990. Silurian orogeny in the Newfoundland Appalachians. J. Geol. 98, 895–913. https://doi.org/10.1086/629460.

Enachescu, M.E., 1987. Tectonic and structural framework of the northeast Newfoundland continental margin. In: Beaumont, C., Tankard, A.J. (Eds.), Sedimentary Basins and Basin-Forming Mechanisms, vol. 12. Canadian Society of Petroleum Geologists Memoir, pp. 117–146. https://doi.org/10.1144/SP369.15.

Falvey, D.A., 1974. The development of continental margins in plate tectonic theory. J. Austr. Petrol. Prod. Explor. Assoc. 14, 95–106. https://doi.org/10.1071/AJ73012.

Feely, M., Wilton, D.H., Costanzo, A., Kollar, A.D., Goudie, D.J., Joyce, A., 2019. Mineral liberation analysis and scanning electron microscopy of Connemara marble: new mineral distribution maps of an iconic Irish gem material. J. Gemmol. 36, 456–466. https://doi.org/10.15506/JoG.2019.36.5.456.

Fernández-Suárez, J., Dunning, G.R., Jenner, G.A., Gutiérrez-Alonso, G., 2000. Variscan collisional magmatism and deformation in NW Iberia: constraints from U-Pb geochronology of granitoids. J. Geol. Soc. 157, 565–576. https://doi.org/10.1144/jgs.157.3.565.

Fisher, C.M., Vervoort, J.D., DuFrane, S.A., 2014. Accurate Hf isotope determinations of complex zircons using the "laser ablation split stream" method. G-cubed 15, 121–139. https://doi.org/10.1002/2013GC004962.

Fisher, C.M., Paton, C., Pearson, D.G., Sarkar, C., Luo, Y., Tersmette, D.B., Chacko, T., 2017. Data reduction of laser ablation split-stream (LASS) analyses using newly developed features within Iolite: with applications to Lu-Hf + U-Pb in detrital zircon and Sm-Nd + U-Pb in igneous monazite. G-cubed 18, 4604–4622. https://doi.org/10.1002/2017GC007187.

Force, E.R., Barr, S.M., 2012. Provenance of the lower Carboniferous Horton Group, Petit-de-Grat Island, Nova Scotia, as revealed by detrital zircon ages. Atl. Geol. 48, 137–145. https://doi.org/10.4138/atlgeol.2012.007.

Foster, D.G., Robinson, A.G., 1993. Geological history of the Flemish Pass basin, offshore Newfoundland. AAPG (Am. Assoc. Pet. Geol.) Bull. 77, 588–609. https://doi.org/10.1306/BDFF8CA4-1718-11D7-8645000102C1865D.

Franke, D., 2013. Rifting, lithosphere breakup and volcanism: comparison of magma-poor and volcanic rifted margins. Mar. Petrol. Geol. 43, 63–87. https://doi.org/10.1016/j.marpetgeo.2012.11.003.

Grange, M., Schärer, U., Cornen, G., Girardeau, J., 2008. First alkaline magmatism during Iberia-Newfoundland rifting. Terra Nova 20, 494–503. https://doi.org/10.1111/j.1365-3121.2008.00847.x.

Grant, D.C., Goudie, D.J., Voisey, C., Shaffer, M., Sylvester, P., 2018. Discriminating hematite and magnetite via Scanning Electron Microscope-Mineral Liberation Analyzer in the -200 mesh size fration of iron ores. B. Appl. Earth Sci. 127, 30–37. https://doi.org/10.1080/03717453.2017.1422334.

Gu, Y., 2003. Automated scanning electron based mineral liberation analysis. An introduction to JKMRC/FEI mineral liberation analyzer. J. Miner. Mater. Char. Eng. 2, 33–41. https://doi.org/10.4236/jmmce.2003.21003.

Hart, S.R., Blusztajn, J., 2006. Age and geochemistry of the mafic sills, ODP site 1276, Newfoundland margin. Chem. Geol. 235, 222–237.
Haworth, R.T., Lefort, J.P., 1979. Geophysical evidence for the extent of the Avalon zone in Atlantic Canada. Can. J. Earth Sci. 16, 552–567. https://doi.org/10.1139/e79-050.
Haynes, S.R., Marshall, J., Wathne, E.I., Minielly, G., Mortlock, E., Walderhaug, O., Johnson, T., 2013. Depositional interpretation and reservoir characterization of the tithonian in Mizzen F-09, Flemish Pass basin, Canada. Abstracts of Integration: CSEG, CSPG and CWLS GeoConvention 2013, Calgary 6. Canada, May 6-10, 2013.
Henriques, S.B.A., Neiva, A.M.R., Tajčmanová, L., Dunning, G.R., 2018. Geochemistry and metamorphism of the mourslcas complex, Ossa-Morena/Central Iberian zone boundary, Iberian massif, central Portugal: implications for the Cadomian and Variscan orogenies. Tectonophysics 296–299, 496–512. https://doi.org/10.1016/j.lithos.2017.11.021.
Hildenbrand, A., Marques, F.O., Quidelluer, X., Noronho, F., 2021. Exhumation history of the Variscan orogen in western Iberia as inferred from new K-Ar and $^{40}Ar/^{39}Ar$ data on granites from Portugal. Tectonophysics 812. https://doi.org/10.1016/j.tecto.2021.228863.
Hiscott, R.N., Wilson, R.C.L., Gradstein, F.M., Pujalte, V., García-Mondéjar, J., Boudreau, R.R., Wishart, H.A., 1990. Comparative stratigraphy and subsidence history of Mesozoic rift basins of North Atlantic. AAPG (Am. Assoc. Pet. Geol.) Bull. 74, 60–76. https://doi.org/10.1306/0C9B2213-1710-11D7-8645000102C1865D.
Hiscott, R.N., Marsaglia, K.M., Wilson, R.C.L., Robertson, A.H.F., Karner, G.D., Tucholke, B.E., Pletsch, T., Petschick, R., 2008. Detrital sources and sediment delivery to the early post-rift (Albian-Cenomanian) Newfoundland basin east of the Grand Banks: results from ODP Leg 210. Bull. Can. Petrol. Geol. 56, 69–92. https://doi.org/10.2113/gscpgbull.56.2.69.
Hoffman, P.F., 1988. United States of America, the birth of a craton: Early Proterozoic assembly and growth of Laurentia. Annu. Rev. Earth Planet Sci. 16, 543–603.
Huismans, R., Beaumont, C., 2011. Depth-dependent extension, two-stage breakup and cratonic underplating at rifted margins. Nature 473, 74–78. https://doi.org/10.1038/nature09988.
Huismans, R., Beaumont, C., 2014. Rifted continental margins: the case for depth-dependent extension. Earth Planet Sci. Lett. 407, 148–162. https://doi.org/10.1016/j.epsl.2014.09.032.
Hutter, A.D., Beranek, L.P., 2020. Upper Jurassic to Lower Cretaceous synrift strata in the Terra Nova oil field, Jeanne d'Arc basin, offshore Newfoundland: a new detrital zircon U-Pb-Hf reference frame for the Atlantic Canadian margin. AAPG (Am. Assoc. Pet. Geol.) Bull. 104, 2325–2349. https://doi.org/10.1306/02232018241.
Jagoutz, O., Muntener, O., Manatschal, G., Rubatto, D., Péron-Pinvidic, G., Turrin, B.D., Villa, I.M., 2007. The rift-to-drift transition in the North Atlantic: a stuttering start of the MORB machine? Geol. 35, 1087–1090. https://doi.org/10.1130/G23613A.1.
Kellett, D.A., Rogers, N., McNicoll, V., Kerr, A., van Staal, C., 2014. New age data refine extent and duration of Paleozoic and Neoproterozoic plutonism at Ganderia–Avalonia boundary, Newfoundland. Can. J. Earth Sci. 51, 943–972. https://doi.org/10.1139/cjes-2014-0090.
Ketchum, J.W.F., Jackson, S.E., Culshaw, N.G., Barr, S.M., 2001. Depositional and tectonic setting of the Paleoproterozoic Lower Aillik Group, Makkovik Province, Canada: evolution of a passive margin-foredeep sequence based on petrochemistry and U-Pb (TIMS and LAM-ICP-MS) geochronology. Precambrian Res. 105, 331–356. https://doi.org/10.1016/S0301-9268(00)00118-2.
King, L.H., Fader, G.B., Poole, W.H., Wanless, R.K., 1985. Geological setting and age of the Flemish Cap granodiorite, east of the Grand Banks of Newfoundland. Can. J. Earth Sci. 22, 1286–1298. https://doi.org/10.1139/e85-133.
King, M.T., Welford, J.K., Peace, A.L., 2020. Investigating the role of the Galicia Bank on the formation of the northwest Iberian margin using deformable plate tectonic models. Tectonophysics 789, 228537. https://doi.org/10.1016/j.tecto.2020.228537.
Krogh, T., Strong, D., O'Brien, S., Papezik, V., 1988. Precise U–Pb zircon dates from the Avalon Terrane in Newfoundland. Canadian Journal of Earth Sciences 25 (3), 442–453. https://doi.org/10.1139/e88-045.
Lau, K.W.H., Louden, K.E., Funck, T., Tucholke, B.E., Holbrook, W.S., Hopper, J.R., Larsen, H.C., 2006. Crustal structure across the Grand Banks-Newfoundland Basin continental margin (Part I) - results from a seismic refraction profile. Geophys. J. Int. 167, 127–156. https://doi.org/10.1111/j.1365-246X.2006.02988.x.
Lavier, L.L., Manatschal, G., 2006. A mechanism to thin the continental lithosphere at magma-poor margins. Nature 440, 324–328. https://doi.org/10.1038/nature04608.
Lister, G.S., Etheridge, M.A., Symonds, P.A., 1986. Detachment faulting and the evolution of passive continental margins. Geol. 14, 246–250. https://doi.org/10.1130/0091-7613(1986)14<246:DFATEO>2.0.CO;2.
Lowe, D.G., Sylvester, P.J., Enachescu, M.E., 2011. Provenance and paleodrainage patterns of Upper Jurassic and Lower Cretaceous synrift sandstones in the Flemish Pass basin, offshore Newfoundland, east coast of Canada. AAPG (Am. Assoc. Pet. Geol.) Bull. 95, 1295–1320. https://doi.org/10.1306/12081010005.
Manatschal, G., 2004. New models for evolution of magma-poor rifted margins based on a review of data and concepts from West Iberia and the Alps. Int. J. Earth Sci. 93, 432–466. https://doi.org/10.1007/s00531-004-0394-7.
Mata, J., Alves, C.F., Martins, L., Miranda, R., Madeira, J., Pimentel, N., Martins, S., Azevedo, M.R., Youbi, N., De Min, A., Almeida, I.M., Bensalah, M.K., Terrinha, P., 2015. $^{40}Ar/^{39}Ar$ ages and petrogenesis of the West Iberian Margin onshore magmatism at the Jurassic-Cretaceous transition: geodynamic implications and assessment of open-system processes involving saline materials. Lithos 236–237, 145–172. https://doi.org/10.1016/j.lithos.2015.09.001.
Matthews, W.A., Guest, B., 2016. A practical approach for collecting large-*n* detrital zircon U-Pb datasets by quadrupole LA-ICP-MS. Geostand. Geoanal. Res. 41, 161–180. https://doi.org/10.1111/ggr.12146.
McDonough, M.R., Sylvester, P., Bruder, N., Lo, J., O'Sullivan, P., 2011. Provenance of reservoir sandstones in the Flemish Pass and Orphan basins (Canada): U-Pb dating of detrital zircons using the laser ablation method. In: Central North Atlantic Conjugate Margins Conference, Lisbon, Portugal, vol. 5, pp. 181–184. September 29–October 1, 2010.
Müntener, O., Manatschal, G., 2006. High degrees of melt extraction recorded by spinel harzburgite of the Newfoundland margin: the role of inheritance and consequences for the evolution of the southern North Atlantic. Earth Planet Sci. Lett. 252, 437–452. https://doi.org/10.1016/j.epsl.2006.10.009.
Murphy, J.B., Hamilton, M.A., 2000. Orogenesis and basin development: U-Pb detrital zircon age constraints on evolution of the late Paleozoic St. Marys basin, central mainland Nova Scotia. J. Geol. 108, 53–71. https://doi.org/10.1086/314384.
Mutter, J.C., 1993. Margins declassified. Nature 364, 393–394. https://doi.org/10.1038/364393a0.
Neuharth, D., Brune, S., Glerum, A., Heine, C., Welford, J.K., 2021. Formation of continental microplates through rift linkage: numerical modelling and its application to the Flemish Cap and Sao Paulo Plateau. G-cubed 22, e2020GC009615. https://doi.org/10.1029/2020GC009615.
Nirrengarten, M., Manatschal, Tugend, J., Kusnir, N., Sauter, D., 2018. Kinematic evolution of the southern North Atlantic: implications for the formation of hyperextended rift systems. Tectonics 37, 89–118. https://doi.org/10.1002/2017TC004495.
O'Brien, S.J., O'Brien, B.H., Dunning, G.R., Tucker, R.D., 1996. Late Neoproterozoic Avalonian and related peri-Gondwanan rocks of the Newfoundland Appalachians. In: Nance, R.D., Thompson, M.D. (Eds.), Avalonian and Related Peri-Gondwanan Terranes of the Circum-North Atlantic, vol. 304. Geological Society of America Special Paper, pp. 9–28.
O'Brien, S.J., Dunning, G.R., Dube, B., O'Driscoll, C.F., Sparkes, B., Israel, S., Ketchum, J., 2001. New insights into the Neoproterozoic geology of the central Avalon Peninsula (parts of NTS map areas 1N/6, 1N/7, and 1N/3), eastern Newfoundland. Government of Newfoundland and Labrador, Department of Mines and Energy, Geological Survey, Current Research Report 2001-1 169–189.
Paton, C., Hellstrom, J., Paul, B., Woodhead, J., Hergt, J., 2011. Iolite: freeware for the visualisation and processing of mass spectrometric data. J. Anal. At. Spectrom. 26, 2508–2518. https://doi.org/10.1039/c1ja10172b.
Pe-Piper, G., Jansa, L.F., Palacz, Z., 1994. Geochemistry and regional significance of the Early Cretaceous bimodal basalt-felsic associations on Grand Banks, eastern Canada. Geol. Soc. Am. Bull. 106, 1319–1331. https://doi.org/10.1130/0016-7606(1994)106<1319:GARSOT>2.3.CO;2.
Pe-Piper, G., Piper, D.J.W., Jansa, L.F., de Jonge, A., 2007. Early Cretaceous opening of the North Atlantic Oocean: implications of the petrology and tectonic setting of the Fogo Seamounts off the SW Grand Banks, Newfoundland. Geol. Soc. Am. Bull. 119, 712–724. https://doi.org/10.1130/B26008.1.
Peace, A.L., Welford, J.K., Geng, M., Sandeman, H., Gaetz, B.D., Ryan, S.S., 2018. Rift-related magmatism on magma-poor margins: structural and potential-field analyses of the Mesozoic Notre Dame Bay intrusions, Newfoundland, Canada and their link to North Atlantic opening. Tectonophysics 745, 24–45. https://doi.org/10.1016/j.tecto.2018.07.025.
Peace, A.L., Welford, J.K., Dunning, G.R., Sandeman, H.A., Camacho, A., 2019. Episodic magmatism resulting from intermittent rifting of the proto-North Atlantic: insights from new geochronological constraints in Newfoundland, Canada. EGU 2019 - Geophysical Research Abstracts 21, 1. -1.
Pereira, M.F., Chichorro, M., Williams, I.S., Silva, J.B., 2008. Zircon U-Pb geochronology of paragneisses and biotite granites from the SW Iberian Massif (Portugal): evidence for a palaeogeographical link between Ossa-Morena Ediacaran basins and the West African craton. In: Ennih, N., Liegeois, J.-P. (Eds.), The Boundaries of the West African Craton, vol. 297. Geological Society of London Special Publication, pp. 385–408. https://doi.org/10.1144/SP297.18.
Pereira, M.F., Linneman, U., Hofmann, M., Chichorro, M., Solá, A.R., Medina, J., Silva, J.B., 2012. The provenance of late Ediacaran and Early Ordovician siliciclastic rocks in the Southwest Central Iberian Zone: constraints from detrital zircon data on northern Gondwana margin evolution during the late Neoproterozoic. Precambrian Res. 192–195, 166–189. https://doi.org/10.1016/j.precamres.2011.10.019.
Pereira, M.F., Gama, C., Chichorro, M., Silva, J.B., Gutíerrez-Alonso, G., Hofmann, M., Linneman, U., Gärtner, A., 2016. Evidence for multi-cycle sedimentation and provenance constraints from detrital zircon U-Pb ages: Triassic strata of the Lusitanian basin (western Iberia). Tectonophysics 681, 318–331. https://doi.org/10.1016/j.tecto.2015.10.011.
Pereira, R., Alves, T.M., Mata, J., 2017. Alternating crustal architecture in West Iberia: a review of its significance in the context of NE Atlantic rifting. J. Geol. Soc. 174, 522–540. https://doi.org/10.1144/jgs2016-050.
Pérez-Gussinyé, M., Reston, T.J., 2001. Rheological evolution during extension at nonvolcanic rifted margins: onset of serpentinization and development of detachments leading to continental breakup. J. Geophys. Res. 106, 3961–3975. https://doi.org/10.1029/2000JB900325.
Péron-Pinvidic, G., Manatschal, G., 2009. The final rifting evolution at deep magma-poor passive margins from Iberia-Newfoundland: a new point of view. Int. J. Earth Sci. 98, 1581–1597. https://doi.org/10.1007/s00531-008-0337-9.
Péron-Pinvidic, G., Manatschal, G., Osmundsen, P.T., 2013. Structural comparison of archetypal Atlantic rifted margins: a review of observations and concepts. Mar. Petrol. Geol. 43, 21–47. https://doi.org/10.1016/j.marpetgeo.2013.02.002.
Petrus, J.A., Kamber, B.S., 2012. VizualAge: a novel approach to laser ablation ICP-MS U-Pb geochronology data reduction. Geostand. Geoanal. Res. 36, 247–270. https://doi.org/10.1111/j.1751-908X.2012.00158.x.
Piper, D.J., Pe-Piper, G., Tubrett, M., Triantafyllidis, S., Strathdee, G., 2012. Detrital zircon geochronology and polycyclic sediment sources, Upper Jurassic–Lower

Cretaceous of the Scotian basin, southeastern Canada. Can. J. Earth Sci. 49, 540–557. https://doi.org/10.1139/e2012-072.

Rainbird, R.H., Rayner, N.M., Hadlari, T., Heaman, L.M., Ielpi, A., Turner, E.C., MacNaughton, R.B., 2017. Zircon provenance data record the lateral extent of pancontinental, Early Neoproterozoic rivers and erosional unroofing history of the Grenville orogen. Geol. Soc. Am. Bull. 129, 1408–1423. https://doi.org/10.1130/B31695.1.

Ribeiro, A., Quesada, C., Dallmeyer, R.D., 1990. Geodynamic evolution of the Iberian massif. In: Dallmeyer, R.D., Martínez-Garcia, E. (Eds.), Pre-Mesozoic Geology of Iberia. Springer-Verlag, Berlin, Hiedelberg, pp. 397–410.

Rivers, T., 1997. Lithotectonic elements of the Grenville province: review and tectonic implications. Precambrian Res. 86, 117–154. https://doi.org/10.1016/s0301-9268(97)00038-7.

Rodrigues, B., Chew, D.M., Jorge, R.C.G.S., Fernandes, P., Veiga-Pires, C., Oliveira, J.T., 2015. Detrital zircon geochronology of the Carboniferous Baixo Alentejo Flysch Group (south Portugal); constraints on the provenance and geodynamic evolution of the south Portuguese zone. J. Geol. Soc. 172, 294–308. https://doi.org/10.1144/jgs2013-084.

Sandoval, L., Welford, J.K., MacMahon, H., Peace, A.L., 2019. Determining continuous basins across conjugate margins: the east Orphan, Porcupine, and Galicia interior basins of the south north Atlantic Ocean. Mar. Petrol. Geol. 110, 138–161. https://doi.org/10.1016/j.marpetgeo.2019.06.047.

Saylor, J.E., Sundell, K.E., 2016. Quantifying comparison of large detrital geochronology data sets. Geosphere 12, 203–220. https://doi.org/10.1130/GES01237.1.

Saylor, J.E., Jordan, J.C., Sundell, K.E., Wang, X., Wang, S., Deng, T., 2018. Topographic growth of the Jishi Shan and its impact of basin and hydrology evolution, NE Tibetan Plateau. Basin Res. 30, 544–563. https://doi.org/10.1111/bre.12264.

Saylor, J.E., Sundell, K.E., Sharman, G.R., 2019. Characterizing sediment sources by non-negative matrix factorization of detrital geochronological data. Earth Planet Sci. Lett. 512, 46–58. https://doi.org/10.1016/j.epsl.2019.01.044.

Shannon, P.M., Williams, B.P.J., Sinclair, I.K., 1995. Tectonic controls on Upper Jurassic to Lower Cretaceous reservoir architecture in the Jeanne d'Arc basin, with some comparisons from the Porcupine and Moray Firth basins. In: Croker, P.F., Shannon, P.M. (Eds.), The Petroleum Geology of Ireland's Offshore Basins, vol. 93. Geological Society of London Special Publication, pp. 467–490.

Sibuet, J.-C., Tucholke, B.E., 2013. The geodynamic province of transitional lithosphere adjacent to magma-poor continental margins. In: Mohriak, W.U., Danforth, A., Post, P.J., Brown, D.E., Tari, G.C., Nemcok, M., Sinha, S.T. (Eds.), Conjugate Divergent Margins, vol. 369. Geological Society of London Special Publication.

Sibuet, J.-C., Srivastava, S.P., Enachescu, M., Karner, G.D., 2007. Early Cretaceous motion of Flemish Cap with respect to North America: implications on the formation of Orphan basin and SE Flemish Cap-Galicia Bank conjugate margins. In: Karner, G. D., Manatschal, G., Pinheiro, L.M. (Eds.), Imaging, Mapping and Modelling Lithosphere Extension and Breakup, vol. 282. Geological Society of London Special Publication, pp. 63–76.

Sinclair, I.K., 1988. Evolution of Mesozoic-Cenozoic sedimentary basins in the Grand Banks area of Newfoundland and comparison with Falvey's (1974) rift model. Bull. Can. Petrol. Geol. 36, 255–273. https://doi.org/10.35767/gscpgbull.36.3.255.

Sinclair, I.K., 1993. Tectonism: the dominant factor in mid-Cretaceous deposition in the Jeanne d'Arc basin, Grand Banks. Mar. Petrol. Geol. 10, 530–549. https://doi.org/10.1016/0264-8172(93)90058-Z.

Sinclair, I.K., McAlpine, D., Sherwin, D.F., McMillian, N.J., Taylor, G.C., Best, M.E., Campbell, G.R., Hea, J.P., Henao, D., Procter, R.M., 1992. Petroleum resources of the Jeanne d'Arc basin and environs, Grand Banks, Newfoundland. In: Geological Survey of Canada Paper 92-98, pp. 1–45. https://doi.org/10.4095/133671.

Skogseid, J., 2001. Volcanic margins: geodynamic and exploration aspects. Mar. Petrol. Geol. 18, 457–461. https://doi.org/10.1016/S0264-8172(00)00070-2.

Sláma, J., Košler, J., Condon, D.J., Crowley, J.L., Gerdes, A., Hanchar, J.M., Horstwood, M.S.A., Morris, G.A., Nasdala, L., Norberg, N., Schaltegger, U., Schoene, B., Tubrett, M.N., Whitehouse, M.J., 2008. Plešovice zircon – a new natural reference material for U-Pb and Hf isotopic microanalysis. Chem. Geol. 249, 1–35. https://doi.org/10.1016/j.chemgeo.2007.11.005.

Soares, D.M., Alves, T.M., Terrinha, P., 2012. The breakup sequence and associated lithospheric breakup surface: their significance in the context of rifted continental margins (West Iberia and Newfoundland margins, North Atlantic. Earth Planet Sci. Lett. 355, 311–326. https://doi.org/10.1016/j.epsl.2012.08.036.

Soares, D.M., Alves, T.M., Terrinha, P., 2014. Contourite drifts on early passive margins as an indicator of established lithospheric breakup. Earth Planet Sci. Lett. 401, 116–131. https://doi.org/10.1016/j.epsl.2014.06.001.

Söderlund, U., Patchett, P.J., Vervoort, J.D., Isachsen, C.E., 2004. The ^{176}Lu decay constant determined by Lu-Hf and U-Pb isotope systematics of Precambrian mafic intrusions. Earth Planet Sci. Lett. 219, 311–324. https://doi.org/10.1016/S0012821X(04)00012-3.

Solá, A.R., Pereira, M.F., Williams, I.S., Ribeiro, M.L., Neiva, A.M.R., Montero, P., Bea, F., Zinger, T., 2008. New insights from U-Pb zircon dating of Early Ordovician magmatism on the northern Gondwana margin: the Urra Formation (SW Iberian massif, Portugal). Tectonophysics 461, 114–129. https://doi.org/10.1016/j.tecto.2008.01.011.

Spencer, C.J., Kirkland, C.L., Taylor, R.J.M., 2016. Strategies towards statistically robust interpretations of in situ U-Pb zircon geochronology. Geosci. Front. 7, 581–589. https://doi.org/10.1016/j.gsf.2015.11.006.

Srivastava, S.P., Sibuet, J.-C., Cande, S., Roest, W.R., Reid, I.D., 2000. Magnetic evidence for slow seafloor spreading during formation of the Newfoundland and Iberian margins. Earth Planet Sci. Lett. 182, 61–76. https://doi.org/10.1016/S0012-821X(00)00231-4.

Srivastava, S.P., Verhoef, J., 1992. Evolution of Mesozoic sedimentary basins around the North Central Atlantic: a preliminary plate kinematic solution. In: Parnell, J. (Ed.), Basins on the Atlantic Seaboard: Petroleum Geology, Sedimentology and Basin Evolution, vol. 62. Geological Society of London Special Publication, pp. 397–420. https://doi.org/10.1144/GSL.SP.1992.062.01.30.

Sundell, K., Saylor, J.E., Pecha, M., 2019. Provenance and recycling of detrital zircons from Cenozoic Altiplano strata and the crustal evolution of western South America from combined U-Pb and Lu-Hf isotopic analysis. In: Horton, B., Folguera, A. (Eds.), Andean Tectonics. Elsevier, Amsterdam, pp. 363–397. https://doi.org/10.1016/B978-0-12-816009-1.00014-9.

Sutra, E., Manatschal, G., 2012. How does the continental crust thin in a hyperextended rifted margin? Insights from the Iberia margin. Geol. 40, 139–142. https://doi.org/10.1130/G32786.1.

Sutra, E., Manatschal, G., Mohn, G., Unternehr, P., 2013. Quantification and restoration of extensional deformation along the Western Iberia and Newfoundland rifted margins. G-cubed 14, 2575–2597. https://doi.org/10.1002/ggge.20135.

Sylvester, P.J., 2012. Use of the mineral liberation analyzer (MLA) for mineralogical studies of sediments and sedimentary rocks. In: Sylvester, P. (Ed.), Quantitative Mineralogy and Microanalysis of Sediments and Sedimentary Rocks. Mineralogical Association of Canada Short Course 42, pp. 1–16. Quebec, Canada.

Tankard, A.J., Welsink, H.J., 1987. Extensional tectonics and stratigraphy of Hibernia oil field, Grand Banks, Newfoundland. AAPG (Am. Assoc. Pet. Geol.) Bull. 71, 1210–1232. https://doi.org/10.1306/703C804C-1707-11D7-8645000102C1865D.

Tucholke, B.E., Sibuet, J.C., 2007. Leg 210 synthesis: tectonic, magmatic, and sedimentary evolution of the Newfoundland-Iberia rift. In: Proc. ODP, Sci. Results, vol. 210, pp. 1–56 (College Station, TX).

Tucholke, B.E., Sawyer, D.S., Sibuet, J.-C., 2007. Breakup of the Newfoundland-Iberia rift. In: Karner, G., Manatschal, G., Pinheiro, L.D. (Eds.), Imaging, Mapping and Modelling Continental Lithosphere Extension and Breakup, vol. 282. Geological Society of London Special Publication, London, pp. 9–46. https://doi.org/10.1144/SP282.2.

Tugend, J., Gillard, M., Manatschal, G., Nirrengarten, M., Harkin, C., Epin, M.E., Sauter, D., Autin, J., Kusznir, N., McDermott, K., 2020. Reappraisal of the magma-rich versus magma-poor rifted margin archetypes. In: McClay, K.R., Hammerstein, J. A. (Eds.), Passive Margins: Tectonics, Sedimentation, and Magmatism, vol. 476. Geological Society of London Special Publication, pp. 23–47. https://doi.org/10.1144/SP476.9.

Valverde-Vaquero, P., Dunning, G., 2000. New U-Pb ages for Early Ordovician magmatism in central Spain. J. Geol. Soc. 157, 15–26. https://doi.org/10.1144/jgs.157.1.15.

Valverde-Vaquero, P., van Staal, C.R., McNicoll, V., Dunning, G., 2006. Mid – Late Ordovician magmatism and metamorphism along the Gander margin in central Newfoundland. J. Geol. Soc. 163, 347–362. https://doi.org/10.1144/0016-764904-130.

Van Avendonk, H.J.A., Holbrook, W.S., Nunes, G.T., Shillington, D.J., Tucholke, B.E., Louden, K.E., Larsen, H.C., Hopper, J.R., 2006. Seismic velocity structure of the rifted margin of the eastern Grand Banks of Newfoundland, Canada. J. Geophys. Res. 111, B11404 https://doi.org/10.1029/2005JB004156.

van Staal, C.R., Barr, S.M., McClausland, P.J.A., Thompson, M.D., White, C.E., 2021a. Tonian-Ediacaran tectonomagmatic evolution of West Avalonia and its Ediacaran-early Cambrian interactions with Ganderia: an example of complex terrane transfer due to arc-arc collision?. In: Murphy, J.B., Strachan, R.A., Quesada, C. (Eds.), Pannotia to Pangea, Neoproterozoic and Paleozoic Orogenic Cycles in the Circum-Atlantic Region, vol. 503. Geological Society of London Special Publication, pp. 143–157. https://doi.org/10.1144/SP503-2020-23.

van Staal, C.R., Barr, S.M., Waldron, J.W.F., Schofield, D.I., Zagorevski, A., White, C.E., 2021b. Provenance and tectonic evolution of Ganderia and its relationships with Avalonia and Megumia in the Appalachian-Caledonide orogen. Gondwana Res. 98, 212–243. https://doi.org/10.1016/j.gr.2021.05.025.

Vaughn, A.P.M., Scarrow, J.H., 2003. K-rich mantle metasomatism control of localization and initiation of lithospheric strike-slip faulting. Terra. Nova 15, 163–169. https://doi.org/10.1046/j.1365-3121.2003.00485.x.

Vermeesch, P., 2021. Maximum depositional age estimation revisited. Geosci. Front. 12, 843–850. https://doi.org/10.1016/j.gsf.2020.08.008.

Welford, J.K., Hall, J., 2007. Crustal structure of the Newfoundland rifted continental margin from constrained 3-D gravity inversion. Geophys. J. Int. 171, 890–908. https://doi.org/10.1111/j.1365-246X.2007.03549.x.

Welford, J.K., Smith, J.A., Hall, J., Deemer, S., Srivastava, S.P., Sibuet, J.-C., 2010. Structure and rifting evolution of the northern Newfoundland basin from Erable multichannel seismic reflection profiles across the southeastern margin of Flemish Cap. Geophys. J. Int. 180, 976–998. https://doi.org/10.1111/j.1365-246X.2009.04477.x.

Welford, J.K., Dehler, S.A., Funck, T., 2020. Crustal velocity structure across the Orphan basin and Orphan Knoll to the continent-ocean transition, offshore Newfoundland, Canada. Geophys. J. Int. 221, 37–59. https://doi.org/10.1093/gji/ggz575.

Welsink, H., Tankard, A., 2012. 14-Extensional tectonics and stratigraphy of the mesozoic Jeanne d'Arc basin, Grand Banks of Newfoundland, regional geology and tectonics. In: Roberts, D.G., Bally, A.W. (Eds.), Phanerozoic Rift Systems and Sedimentary Basins. Elsevier, Boston, pp. 336–381. https://doi.org/10.1016/B978-0-444-56356-9.00013-4.

Whitmarsh, R.B., Manatschal, G., Minshull, T.A., 2001. Evolution of magma-poor continental margins from rifting to seafloor spreading. Nature 413, 150–154. https://doi.org/10.1038/35093085.

Whitmeyer, S.J., Karlstrom, K.E., 2007. Tectonic model for the proterozoic growth of north America. Geosphere 3, 220–259. https://doi.org/10.1130/GES00055.1.

Wiedenbeck, M., Alle, P., Corfu, F., Griffin, E., Meier, M., Oberli, F., Von Quadt, A., Roddick, J., Spiegel, W., 1995. Three natural zircon standards for U-Th-Pb, Lu-Hf, trace element and REE analyses. Geostand. Newsl. 19, 1–23. https://doi.org/10.1111/j.1751-908X.1995.tb00147.x.

Willner, A.P., Barr, S.M., Gerdes, A., Massonne, H.J., White, C.E., 2013. Origin and evolution of Avalonia: evidence from U-Pb and Lu-Hf isotopes in zircon from the Mira terrane, Canada, and the Stavelot-Venn massif, Belgium. J. Geol. Soc. 170, 769–784. https://doi.org/10.1144/jgs2012-152.

Xiong, D., Azmy, K., Blamey, N.J.F., 2016. Diagenesis and origin of calcite cement in the Flemish Pass basin sandstone reservoir (Upper Jurassic): implications for porosity development. Mar. Petrol. Geol. 70, 93–118. https://doi.org/10.1016/j.marpetgeo.2015.11.013.

Zhao, F., Berndt, C., Alves, T.M., Xia, S., Li, L., Mi, L., Fan, C., 2021. Widespread hydrothermal vents and associated volcanism record prolonged Cenozoic magmatism in the South China Sea. Geol. Soc. Am. Bull. 133, 2645–2660. https://doi.org/10.1130/B35897.1.